



MICCAI2022

Singapore

25th International Conference on
Medical Image Computing and
Computer Assisted Intervention
September 18-22, 2022
Resorts World Convention Centre Singapore

Learning with Limited Supervision



UC SANTA CRUZ

Yuyin Zhou (Yan Wang)
Ismail Ben Ayed
Jose Dolz
Christian Desrosiers
Marleen de Bruijne
Hoel Kervadec



UNIVERSITY OF CALIFORNIA
SANTA CRUZ

Advancing Medical Image Segmentation via Exploiting Limited Annotation

Yan Wang

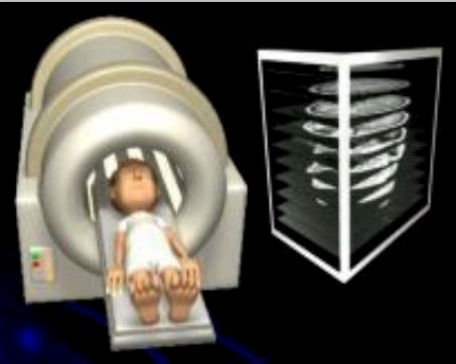
Professor
East China Normal University

Yuyin Zhou

Assistant Professor
University of California, Santa Cruz

Medical Images

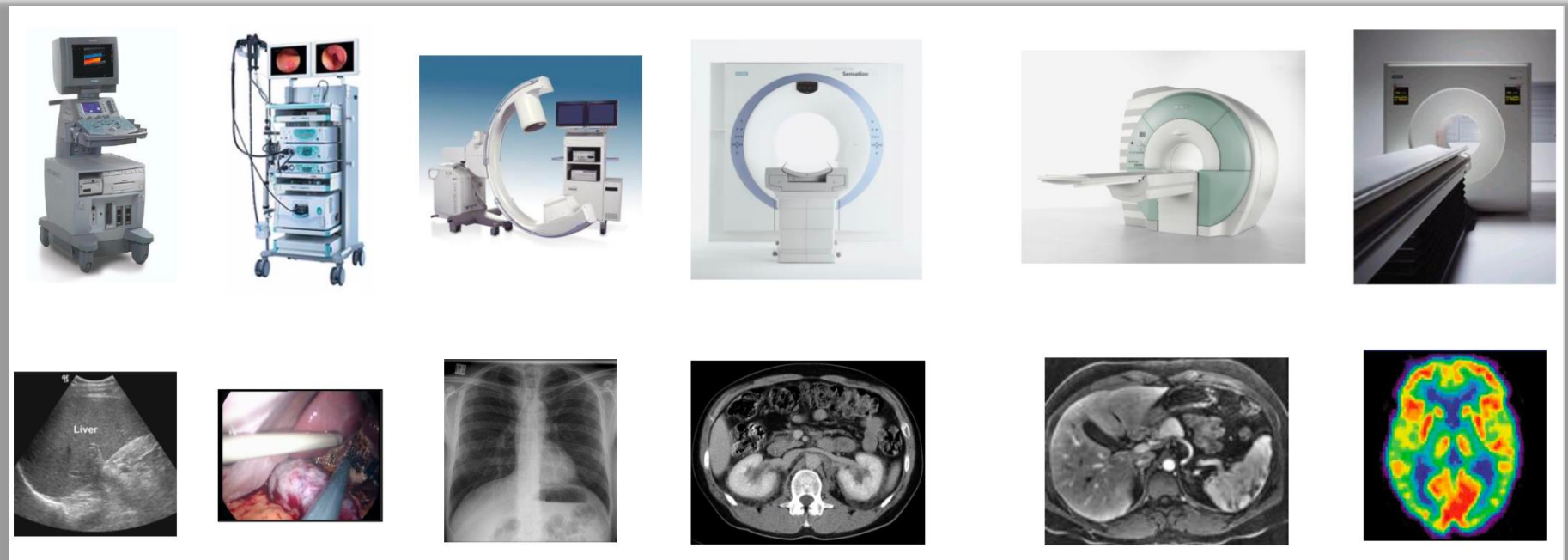
Scanner



Computer



Doctor



Ultrasound

Endoscopy

X-rays

Computed
tomography

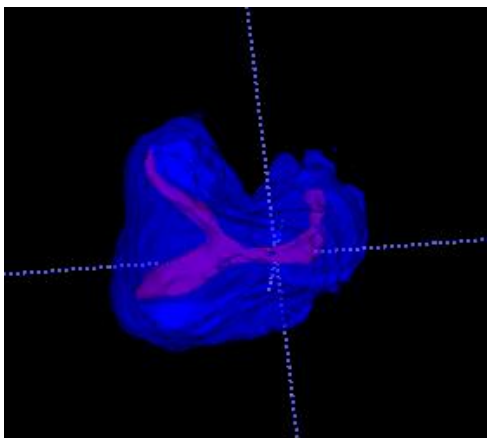
Magnetic
resonance

Positron emission
tomography

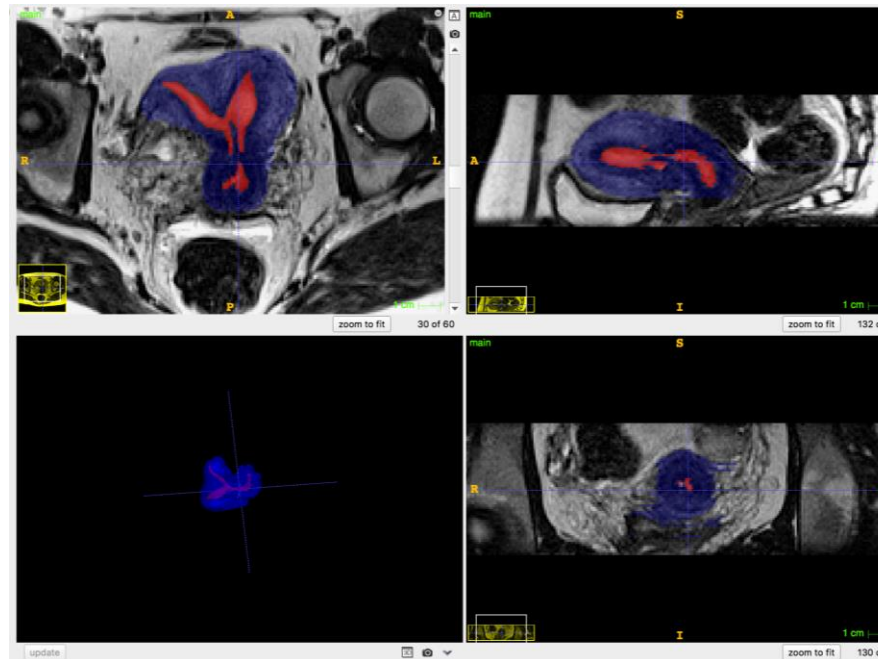
Organ/Lesion Segmentation

Splenic injury

- Clinical applications
 - Computer aided diagnosis
 - Computer aided surgery
 - Radiation therapy



Uterine malformation

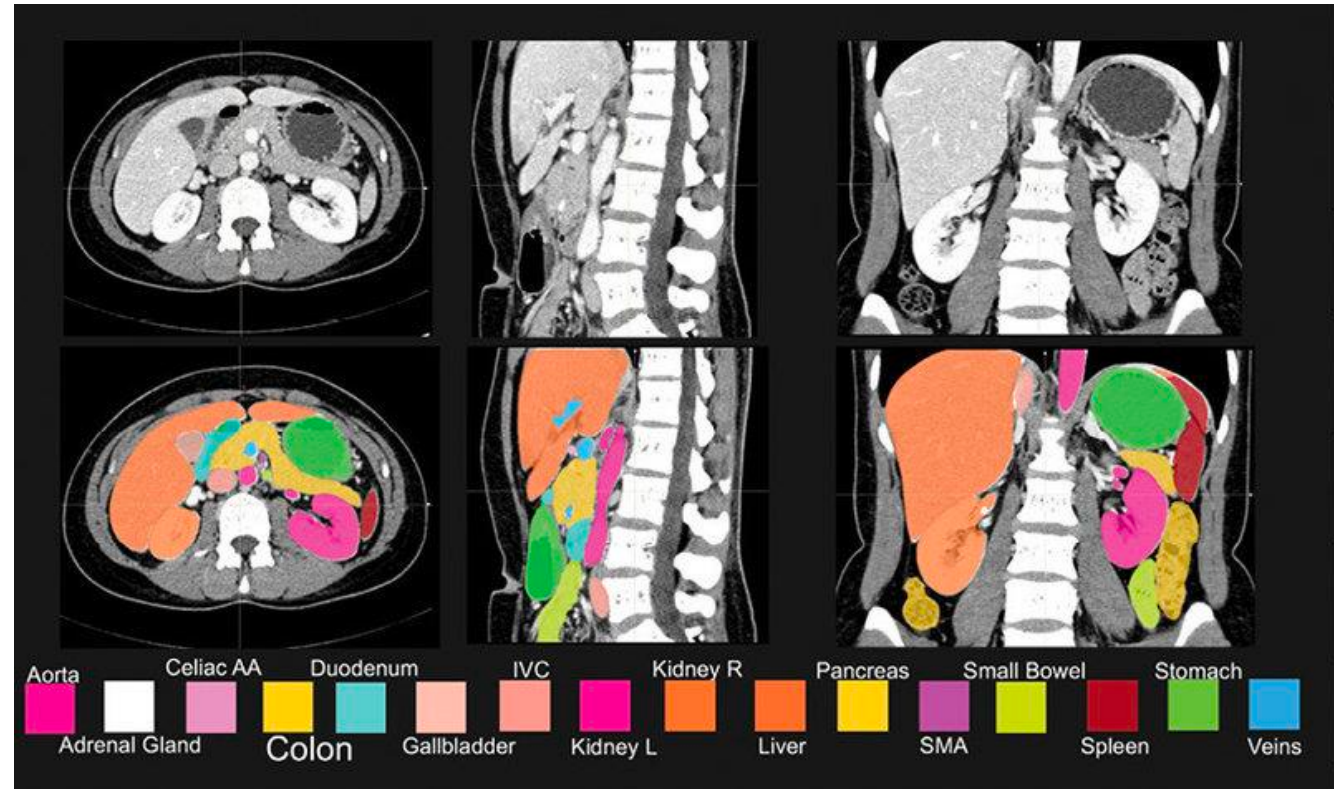


Multi-organ Segmentation

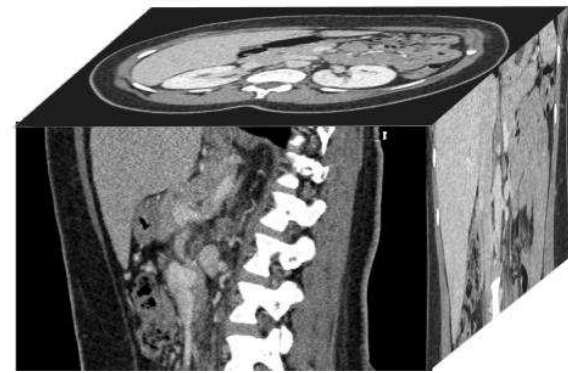
- Data prior:
 - A CT volume can be looked into from three views
 - Patient-wise abdominal organ size distributions are similar

Semi-Supervised 3D Abdominal Multi-Organ Segmentation Via Deep Multi-Planar Co-Training

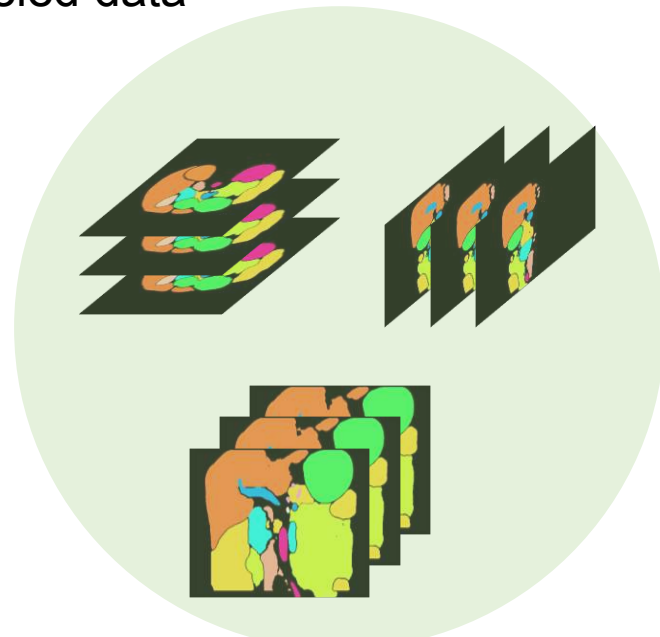
Prior-aware neural network for partially-supervised multi-organ segmentation



Semi-supervised Learning: Deep Multi-Planar Co-Training



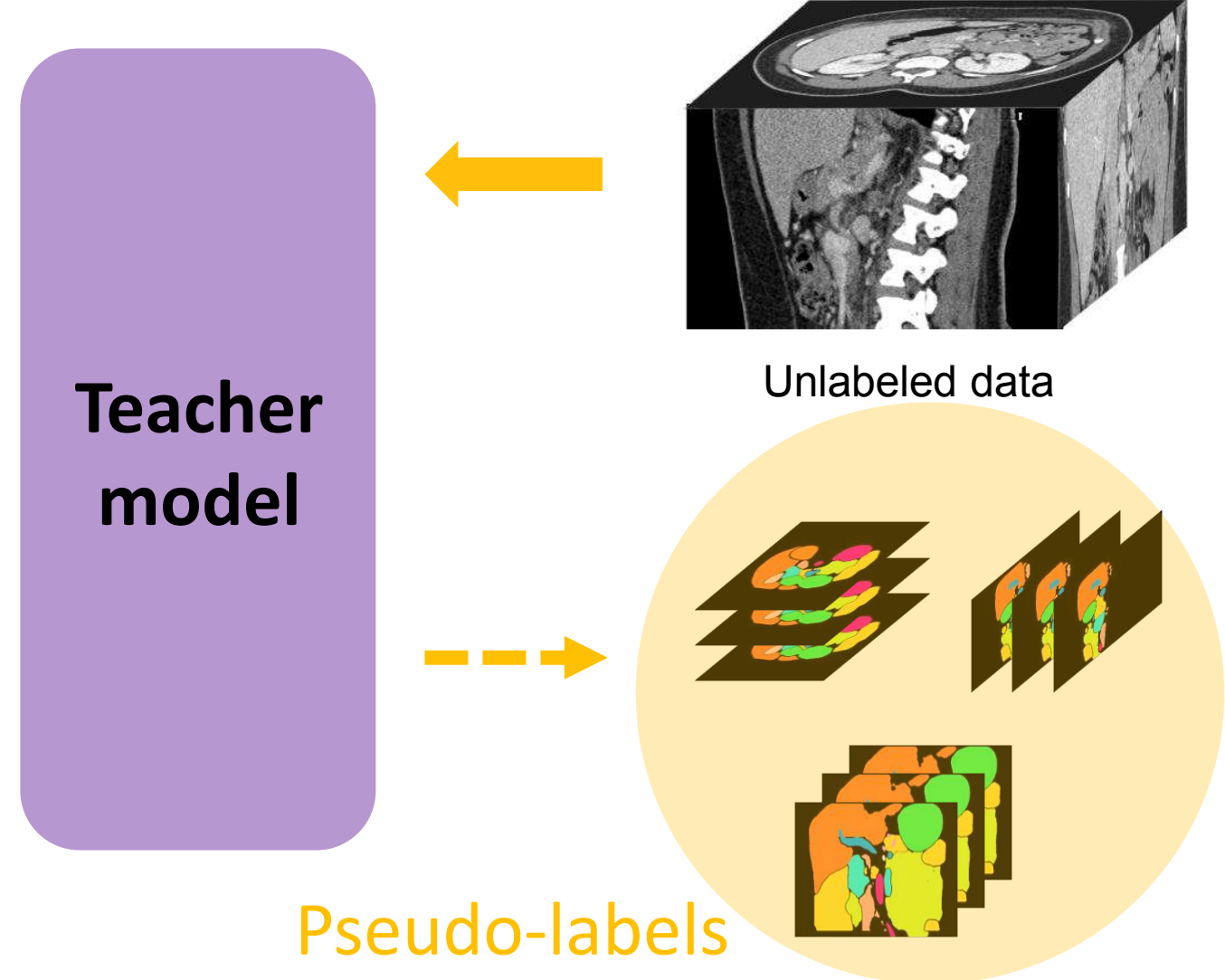
Labeled data



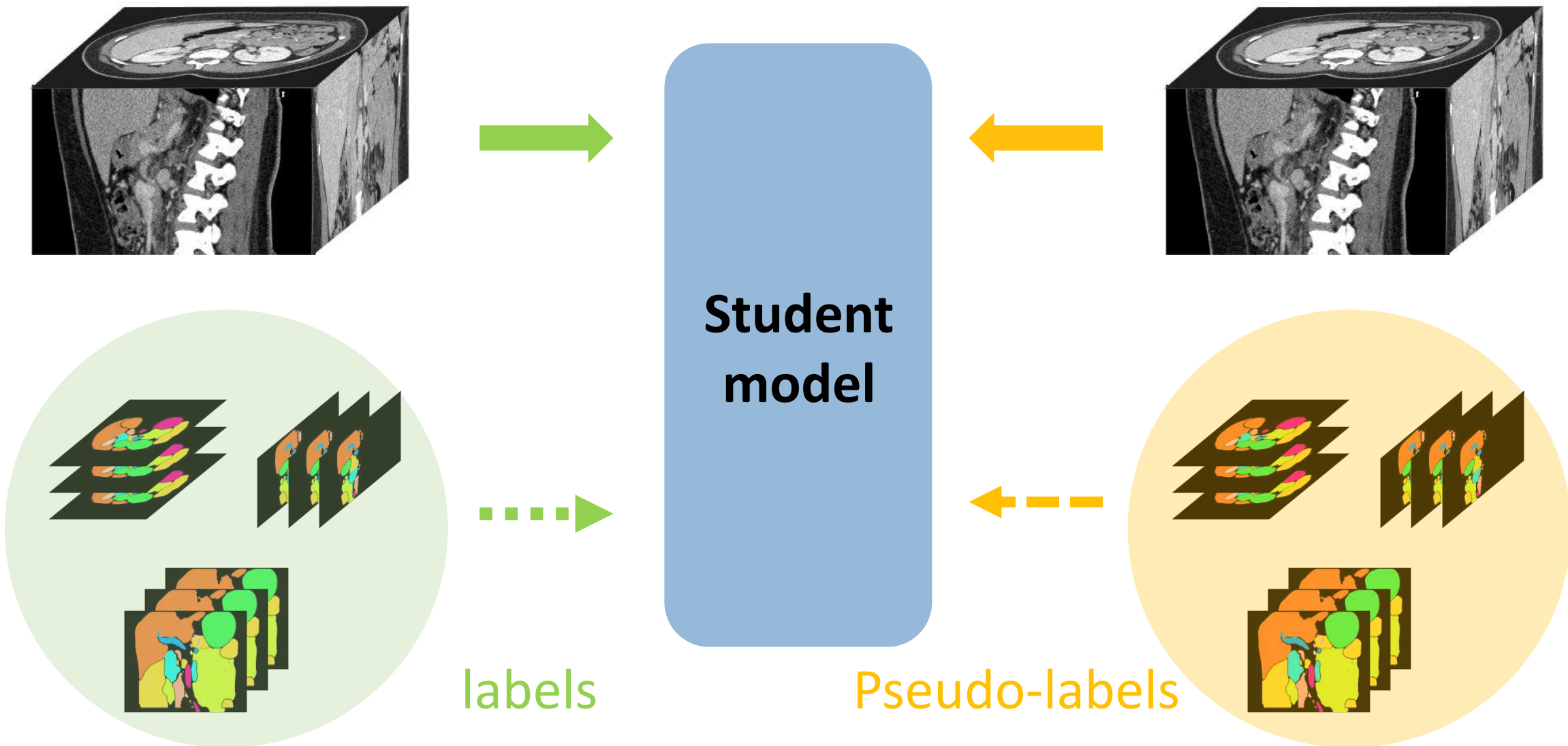
labels



Semi-supervised Learning: Deep Multi-Planar Co-Training



Semi-supervised Learning: Deep Multi-Planar Co-Training



Semi-supervised Learning: Deep Multi-Planar Co-Training

Organ Type	FCN		SPSL		DMPCT (Ours)		<i>p</i> -value
	50 - 0	50 - 50	50 - 100	50 - 50	50 - 100		
Aorta	89.14 ± 7.95	91.10 ± 5.52	90.76 ± 5.90	91.43 ± 4.88	91.54 ± 4.65	3.32×10^{-5}	
Adrenal gland	26.45 ± 12.1	29.92 ± 14.7	26.93 ± 15.6	30.58 ± 12.7	35.48 ± 11.8	1.98×10^{-15}	
Celiac AA	35.01 ± 19.7	37.27 ± 19.0	39.78 ± 18.4	36.25 ± 20.5	40.50 ± 18.9	1.00×10^{-5}	
Colon	71.81 ± 14.9	78.28 ± 13.0	79.58 ± 12.9	79.61 ± 12.3	80.53 ± 11.6	7.69×10^{-12}	
Duodenum	54.89 ± 15.5	57.77 ± 17.3	62.22 ± 14.8	66.95 ± 12.6	64.78 ± 13.8	1.95×10^{-19}	
Gallbladder	86.53 ± 6.21	87.87 ± 5.45	88.02 ± 5.83	88.45 ± 5.07	87.77 ± 6.29	0.002	
IVC	77.67 ± 9.49	81.28 ± 8.87	82.63 ± 7.31	83.49 ± 6.94	83.43 ± 7.02	9.30×10^{-14}	
Kidney (L)	95.12 ± 5.01	95.59 ± 4.97	95.88 ± 3.68	95.82 ± 3.60	96.09 ± 3.42	3.69×10^{-6}	
Kidney (R)	95.69 ± 2.36	95.77 ± 4.93	96.14 ± 2.94	96.17 ± 2.75	96.26 ± 2.29	1.74×10^{-7}	
Liver	95.45 ± 2.41	96.06 ± 0.99	96.07 ± 1.03	96.11 ± 0.97	96.15 ± 0.92	0.005	
Pancreas	76.49 ± 11.6	80.12 ± 7.52	80.93 ± 6.84	81.46 ± 6.32	82.03 ± 6.16	2.97×10^{-8}	
SMA	52.26 ± 17.1	51.81 ± 18.2	51.94 ± 17.1	49.40 ± 19.2	52.70 ± 17.7	0.667	
Small bowel	71.13 ± 13.1	78.93 ± 12.6	79.97 ± 12.8	79.49 ± 12.1	79.25 ± 12.6	2.53×10^{-22}	
Spleen	94.81 ± 2.64	95.46 ± 2.09	95.58 ± 1.90	95.73 ± 2.03	95.98 ± 1.59	1.83×10^{-10}	
Stomach	91.38 ± 3.94	92.62 ± 3.71	92.92 ± 3.65	93.33 ± 3.47	93.42 ± 3.21	3.30×10^{-23}	
Veins	64.75 ± 15.4	70.43 ± 14.3	69.66 ± 14.6	69.82 ± 14.5	70.23 ± 14.4	4.16×10^{-15}	
Mean	73.71 ± 9.97	76.32 ± 9.58	76.87 ± 9.08	77.20 ± 8.75	77.94 ± 8.51	4.74×10^{-90}	

Semi-supervised Learning: Deep Multi-Planar Co-Training

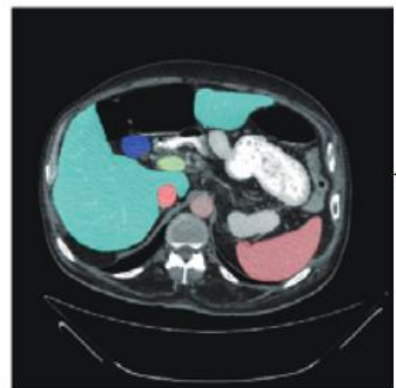
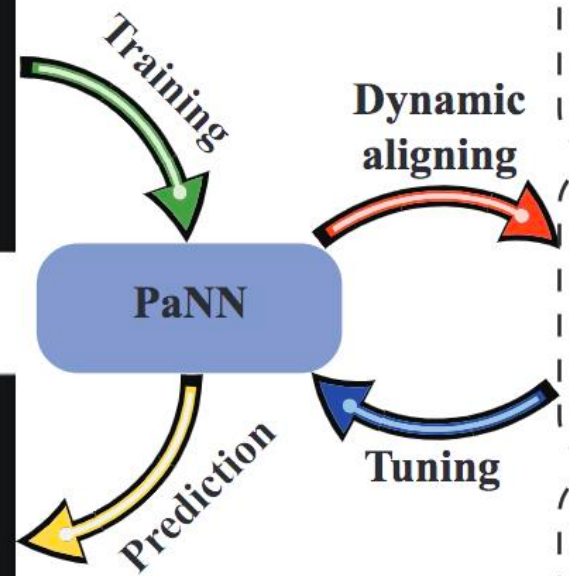
Organ Type	FCN	SPSL		DMPCT (Ours)		<i>p</i> -value
		50 - 50	50 - 100	50 - 50	50 - 100	
	50 - 0					
Aorta	89.14 ± 7.95	91.10 ± 5.52	90.76 ± 5.90	91.43 ± 4.88	91.54 ± 4.65	3.32×10^{-5}
Adrenal gland	26.45 ± 12.1	29.92 ± 14.7	26.93 ± 15.6	30.58 ± 12.7	35.48 ± 11.8	1.98×10^{-15}
Celiac AA	35.01 ± 19.7	37.27 ± 19.0	39.78 ± 18.4	36.25 ± 20.5	40.50 ± 18.9	1.00×10^{-5}
Colon	71.81 ± 14.9	78.28 ± 13.0	79.58 ± 12.9	79.61 ± 12.3	80.53 ± 11.6	7.69×10^{-12}
Duodenum	54.89 ± 15.5	57.77 ± 17.3	62.22 ± 14.8	66.95 ± 12.6	64.78 ± 13.8	1.95×10^{-19}
Gallbladder	86.53 ± 6.21	87.87 ± 5.45	88.02 ± 5.83	88.45 ± 5.07	87.77 ± 6.29	0.002
IVC	77.67 ± 9.49	81.28 ± 8.87	82.63 ± 7.31	83.49 ± 6.94	83.43 ± 7.02	9.30×10^{-14}
Kidney (L)	95.12 ± 5.01	95.59 ± 4.97	95.88 ± 3.68	95.82 ± 3.60	96.09 ± 3.42	3.69×10^{-6}
Kidney (R)	95.69 ± 2.36	95.77 ± 4.93	96.14 ± 2.94	96.17 ± 2.75	96.26 ± 2.29	1.74×10^{-7}
Liver	95.45 ± 2.41	96.06 ± 0.99	96.07 ± 1.03	96.11 ± 0.97	96.15 ± 0.92	0.005
Pancreas	76.49 ± 11.6	80.12 ± 7.52	80.93 ± 6.84	81.46 ± 6.32	82.03 ± 6.16	2.97×10^{-8}
SMA	52.26 ± 17.1	51.81 ± 18.2	51.94 ± 17.1	49.40 ± 19.2	52.70 ± 17.7	0.667
Small bowel	71.13 ± 13.1	78.93 ± 12.6	79.97 ± 12.8	79.49 ± 12.1	79.25 ± 12.6	2.53×10^{-22}
Spleen	94.81 ± 2.64	95.46 ± 2.09	95.58 ± 1.90	95.73 ± 2.03	95.98 ± 1.59	1.83×10^{-10}
Stomach	91.38 ± 3.94	92.62 ± 3.71	92.92 ± 3.65	93.33 ± 3.47	93.42 ± 3.21	3.30×10^{-23}
Veins	64.75 ± 15.4	70.43 ± 14.3	69.66 ± 14.6	69.82 ± 14.5	70.23 ± 14.4	4.16×10^{-15}
Mean	73.71 ± 9.97	76.32 ± 9.58	76.87 ± 9.08	77.20 ± 8.75	77.94 ± 8.51	4.74×10^{-90}

Semi-supervised Learning: Deep Multi-Planar Co-Training

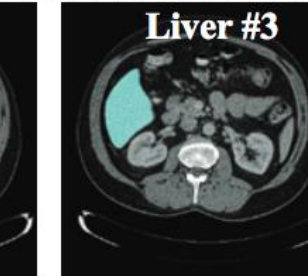
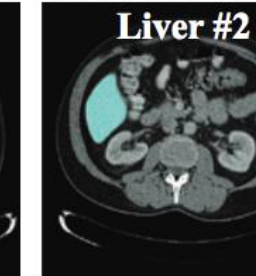
Organ Type	FCN		SPSL		DMPCT (Ours)		<i>p</i> -value
	50 - 0	50 - 50	50 - 100	50 - 50	50 - 100		
Aorta	89.14 ± 7.95	91.10 ± 5.52	90.76 ± 5.90	91.43 ± 4.88	91.54 ± 4.65		3.32×10^{-5}
Adrenal gland	26.45 ± 12.1	29.92 ± 14.7	26.93 ± 15.6	30.58 ± 12.7	35.48 ± 11.8		1.98×10^{-15}
Celiac AA	35.01 ± 19.7	37.27 ± 19.0	39.78 ± 18.4	36.25 ± 20.5	40.50 ± 18.9		1.00×10^{-5}
Colon	71.81 ± 14.9	78.28 ± 13.0	79.58 ± 12.9	79.61 ± 12.3	80.53 ± 11.6		7.69×10^{-12}
Duodenum	54.89 ± 15.5	57.77 ± 17.3	62.22 ± 14.8	66.95 ± 12.6	64.78 ± 13.8		1.95×10^{-19}
Gallbladder	86.53 ± 6.21	87.87 ± 5.45	88.02 ± 5.83	88.45 ± 5.07	87.77 ± 6.29		0.002
IVC	77.67 ± 9.49	81.28 ± 8.87	82.63 ± 7.31	83.49 ± 6.94	83.43 ± 7.02		9.30×10^{-14}
Kidney (L)	95.12 ± 5.01	95.59 ± 4.97	95.88 ± 3.68	95.82 ± 3.60	96.09 ± 3.42		3.69×10^{-6}
Kidney (R)	95.69 ± 2.36	95.77 ± 4.93	96.14 ± 2.94	96.17 ± 2.75	96.26 ± 2.29		1.74×10^{-7}
Liver	95.45 ± 2.41	96.06 ± 0.99	96.07 ± 1.03	96.11 ± 0.97	96.15 ± 0.92		0.005
Pancreas	76.49 ± 11.6	80.12 ± 7.52	80.93 ± 6.84	81.46 ± 6.32	82.03 ± 6.16		2.97×10^{-8}
SMA	52.26 ± 17.1	51.81 ± 18.2	51.94 ± 17.1	49.40 ± 19.2	52.70 ± 17.7		0.667
Small bowel	71.13 ± 13.1	78.93 ± 12.6	79.97 ± 12.8	79.49 ± 12.1	79.25 ± 12.6		2.53×10^{-22}
Spleen	94.81 ± 2.64	95.46 ± 2.09	95.58 ± 1.90	95.73 ± 2.03	95.98 ± 1.59		1.83×10^{-10}
Stomach	91.38 ± 3.94	92.62 ± 3.71	92.92 ± 3.65	93.33 ± 3.47	93.42 ± 3.21		3.30×10^{-23}
Veins	64.75 ± 15.4	70.43 ± 14.3	69.66 ± 14.6	69.82 ± 14.5	70.23 ± 14.4		4.16×10^{-15}
Mean	73.71 ± 9.97	76.32 ± 9.58	76.87 ± 9.08	77.20 ± 8.75	77.94 ± 8.51		4.74×10^{-90}

Partially-supervised Multi-organ Segmentation

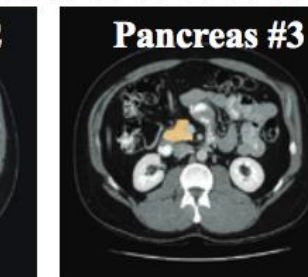
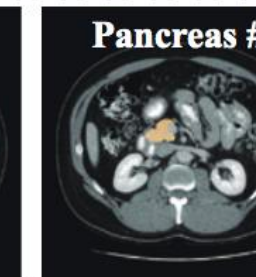
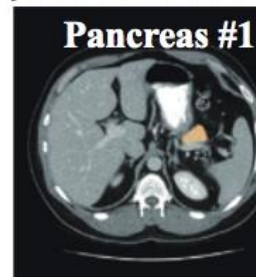
Small fully-labeled dataset



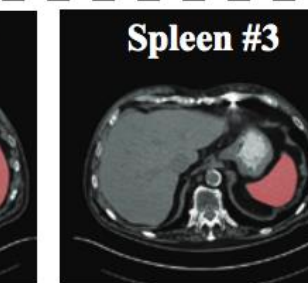
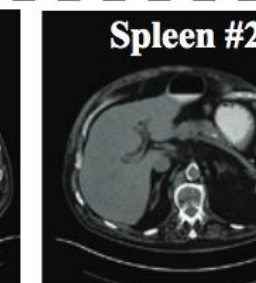
More partially labeled datasets



...



...



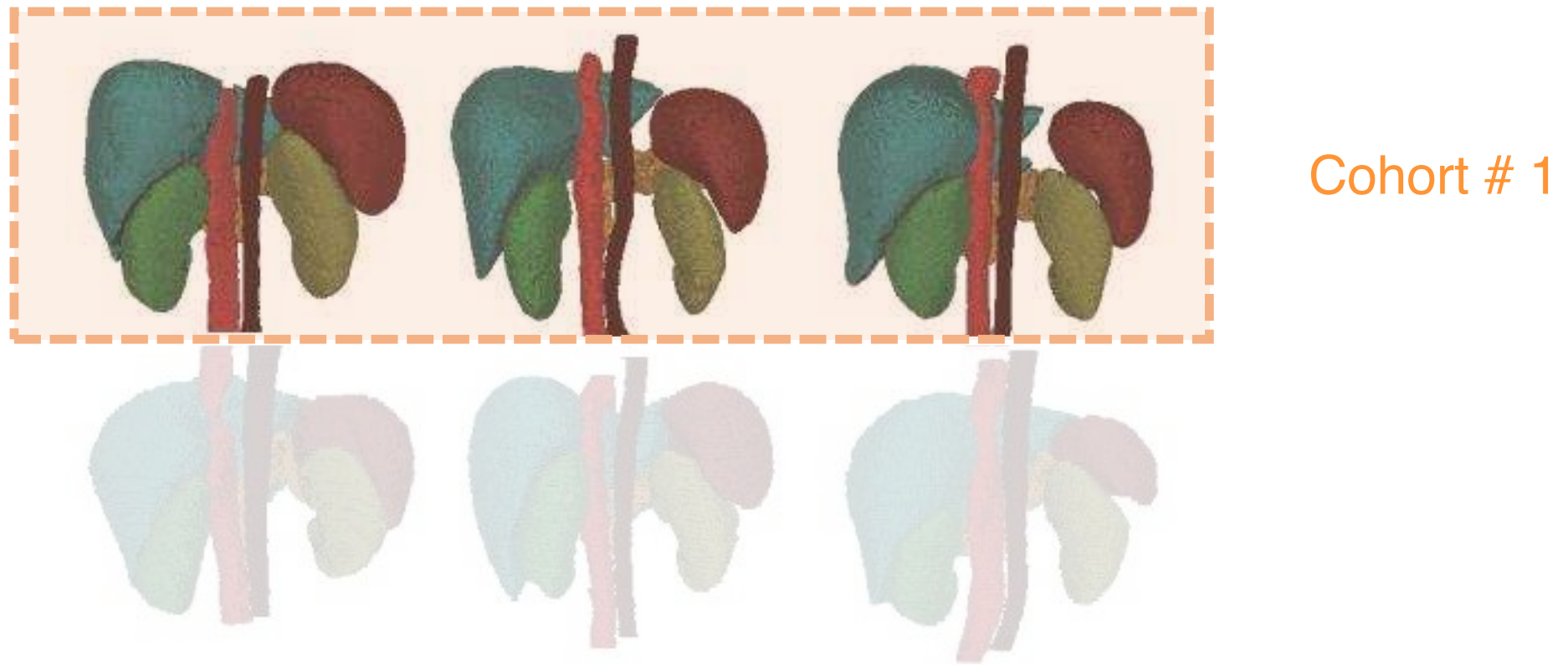
...

Liver
Stomach
Aorta
Esophagus
Gallbladder
Spleen
Kidney(R)
Kidney(L)
Pancreas
IVC
AG(R)
AG(L)
P&S Vein

Yuyin Zhou, Zhe Li, Song Bai, Xinlei Chen, Mei Han, Chong Wang, Elliot K. Fishman, Alan L. Yuille
Prior-aware neural network for partially-supervised multi-organ segmentation, ICCV, 2019.

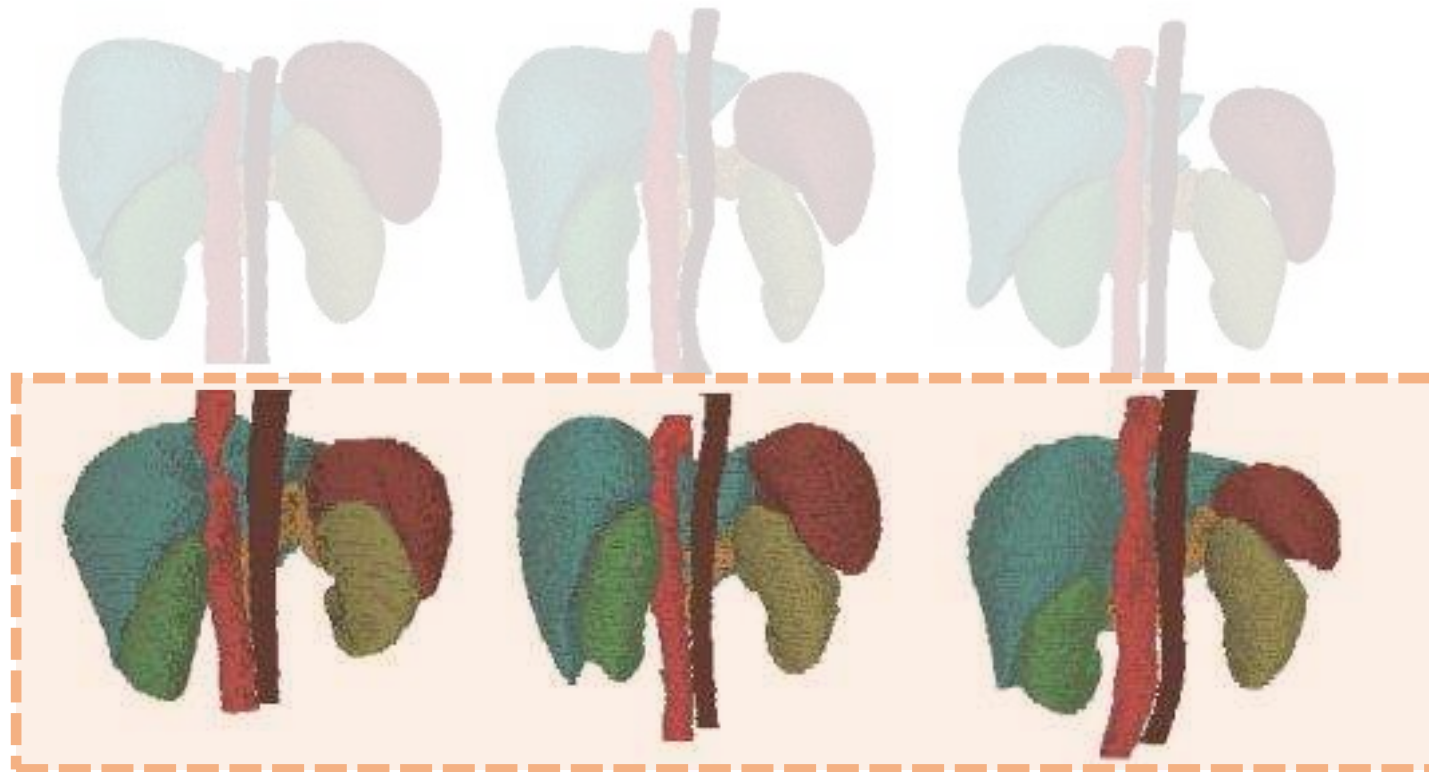
Data Prior: Size

- What is size prior?
 - The similarity of patient-wise abdominal organ size distributions



Data Prior: Size

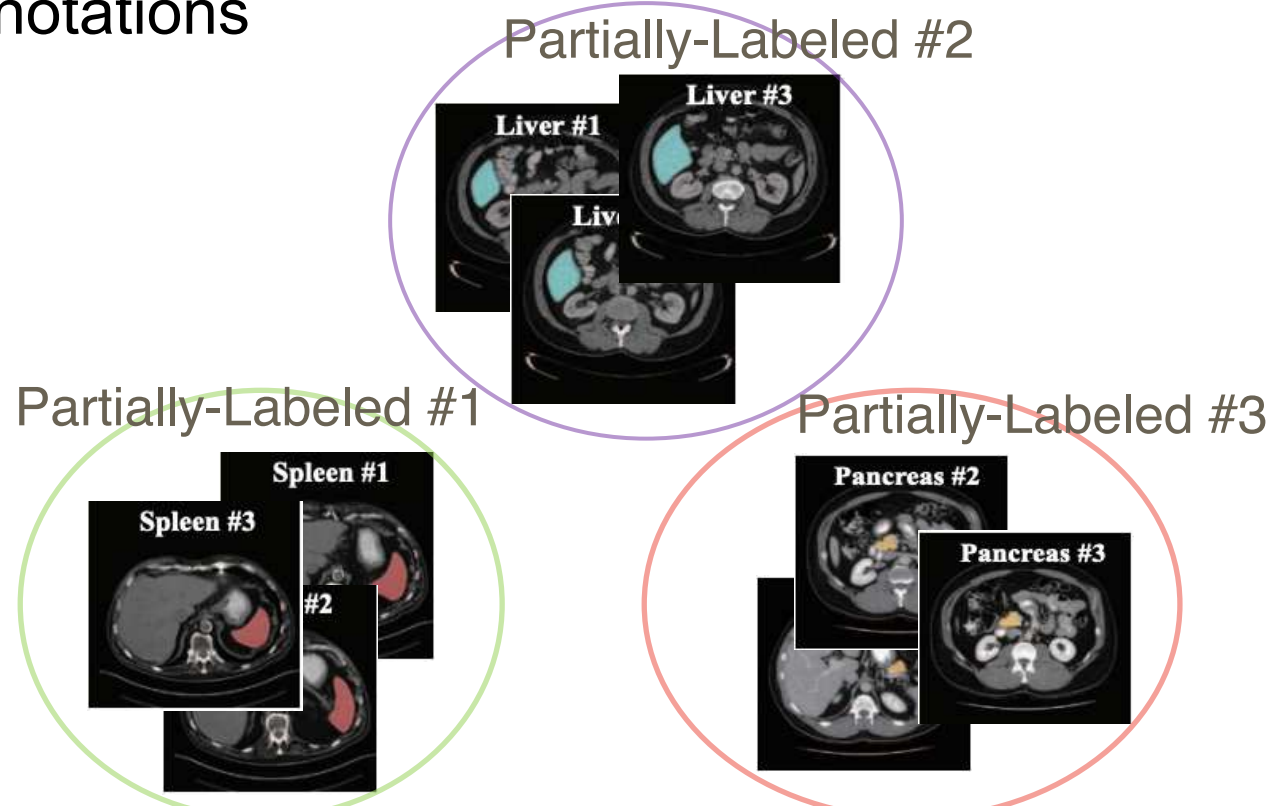
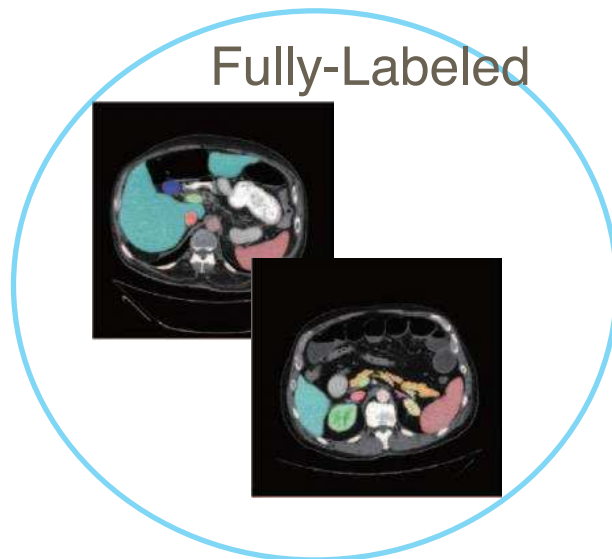
- What is size prior?
 - The similarity of patient-wise abdominal organ size distributions



Partially-supervised Multi-organ Segmentation

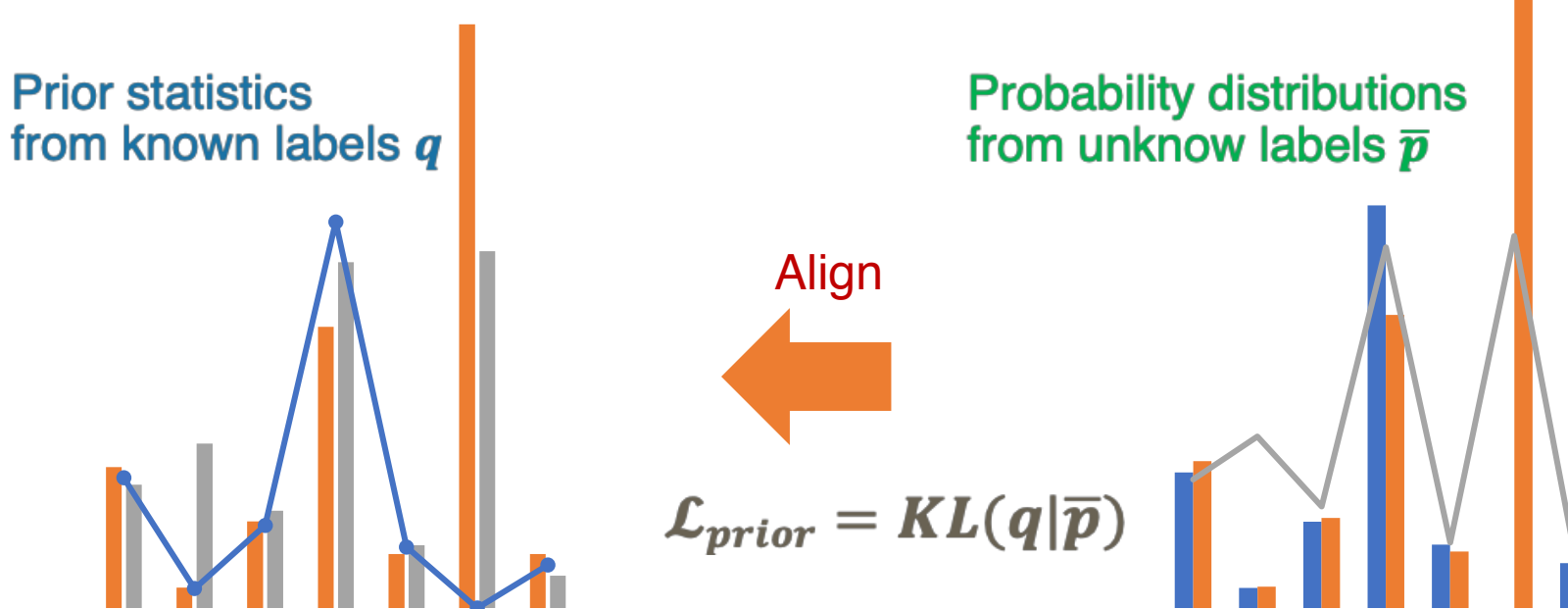
■ Why size prior?

- To mitigate dataset biases
 - Different imaging scanners, populations, etc.
- To handle imperfect annotations



Partially-supervised Multi-organ Segmentation

- How to exploit size prior?
 - Prior-aware loss



Partially-supervised Multi-organ Segmentation

- How to exploit size prior?
 - Prior-aware loss

$$\mathcal{L}_{prior} = KL(q|\bar{p})$$

- Overall loss function

$$\mathcal{L}_{total} = \mathcal{L}_{sup}(\theta) + \lambda_1 \cdot \mathcal{L}_{unsup}(\theta; \hat{y}) + \lambda_2 \cdot \mathcal{L}_{prior}$$

Computed on known labels

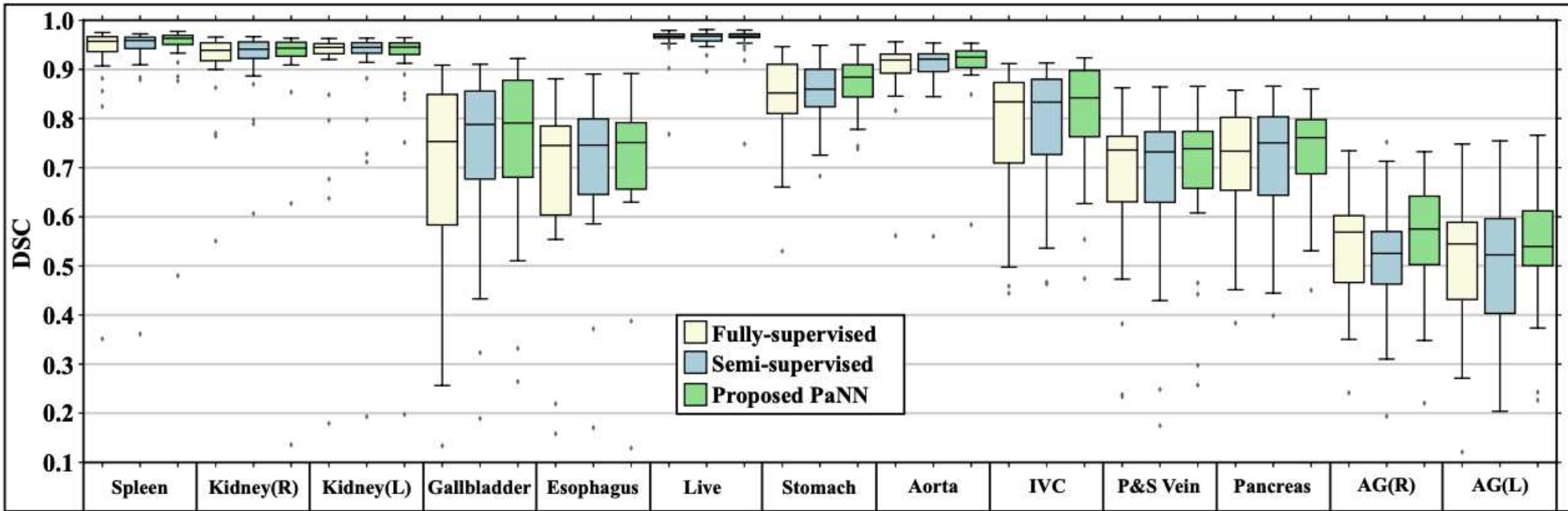
Computed on unknown labels

Balanced weights

```
graph LR; Ltotal["L_total = L_sup(theta) + λ₁ · L_unsup(theta; y-hat) + λ₂ · L_prior"] -- "Computed on known labels" --> Lsup["L_sup(theta)"]; Ltotal -- "Balanced weights" --> Lunsup["L_unsup(theta; y-hat)"]; Ltotal -- "Computed on unknown labels" --> Lprior["L_prior"]
```

Partially-supervised Multi-organ Segmentation

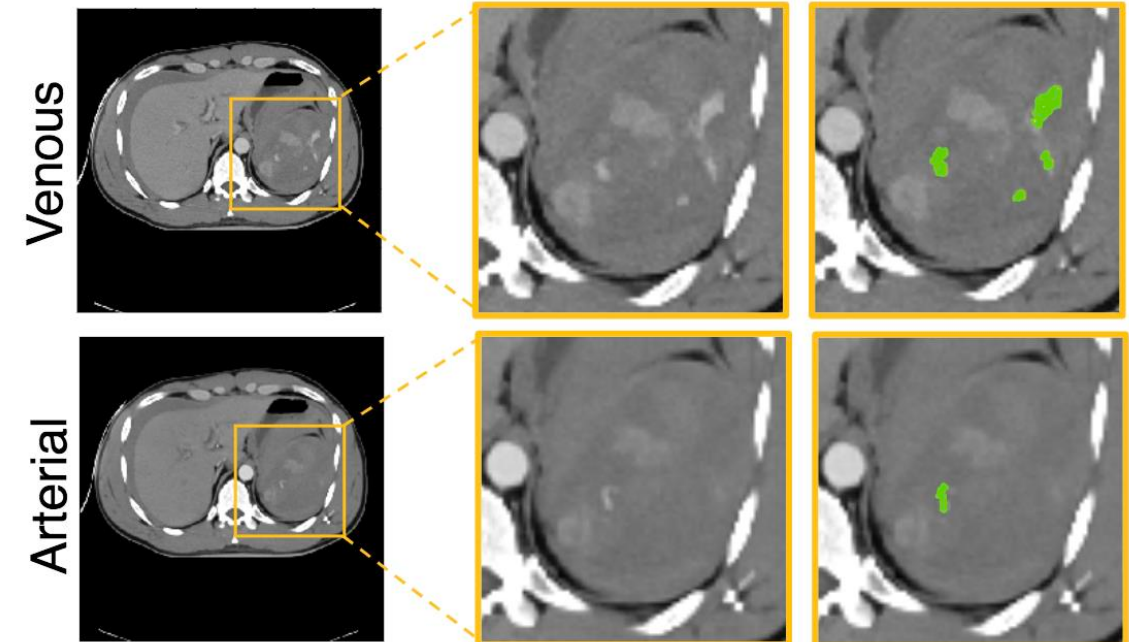
■ Results



Name	Spleen	Kidney(R)	Kidney(L)	Gallbladder	Esophagus	Liver	Aorta	IVC	Average Dice	Mean Surface Distance	Hausdorff Distance
AutoContext3DFCN [33]	0.926	0.866	0.897	0.629	0.727	0.948	0.852	0.791	0.782	1.936	26.095
deedsJointCL [13]	0.920	0.894	0.915	0.604	0.692	0.948	0.857	0.828	0.790	2.262	25.504
dltk0.1_unet_sub2 [28]	0.939	0.895	0.915	0.711	0.743	0.962	0.891	0.826	0.815	1.861	62.872
results_13organs_p0.7	0.890	0.898	0.883	0.685	0.754	0.936	0.870	0.819	0.817	4.559	38.661
PaNN* (ours)	0.961	0.901	0.943	0.704	0.783	0.972	0.913	0.835	0.832	1.641	25.176
PaNN (ours)	0.968	0.920	0.953	0.729	0.790	0.974	0.925	0.847	0.850	1.450	18.468

Lesion/Injury Segmentation

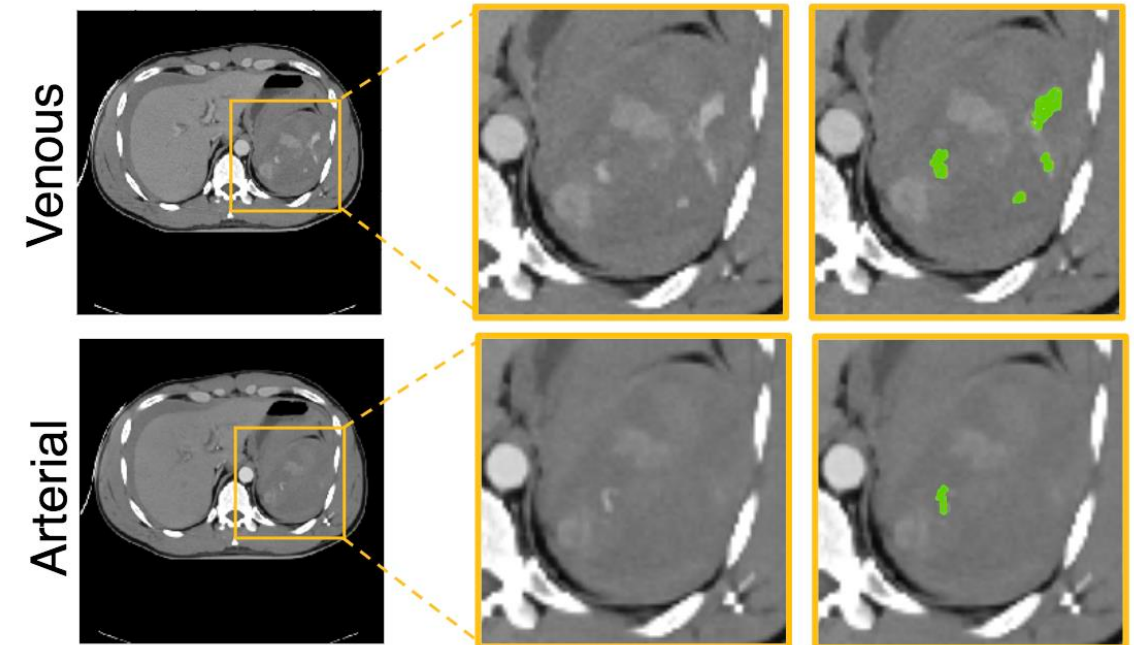
- Attention-guided learning:
 - Exploiting spatial priors as external attention
[External Attention Assisted Multi-Phase Splenic Vascular Injury Segmentation With Limited Data](#)
 - Lesion/tumor region can be considered as attention to bridge classification/segmentation
[Learning Inductive Attention Guidance for Partially Supervised Pancreatic Ductal Adenocarcinoma Prediction](#)



Multi-phase Splenic Vascular Injury Segmentation

Challenges

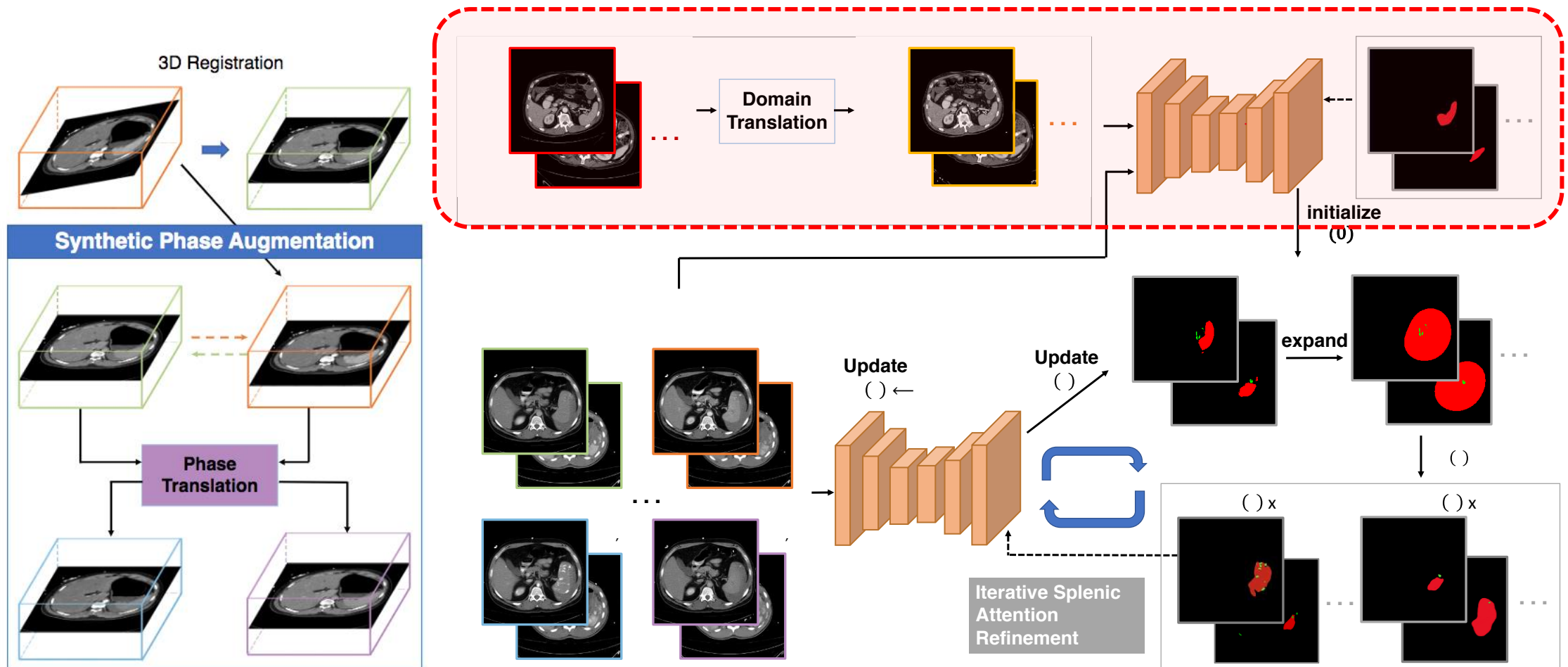
- Highly variant in shape, texture, size and overall appearance
- Extremely small sizes for splenic vascular injury
- Label acquisition is complex and expensive



Yuyin Zhou, David Dreizin, Yan Wang, Fengze Liu, Wei Shen, Alan L. Yuille, External Attention Assisted Multi-Phase Splenic Vascular Injury Segmentation With Limited Data. IEEE Trans. Medical Imaging 41(6): 1346-1357 (2022)

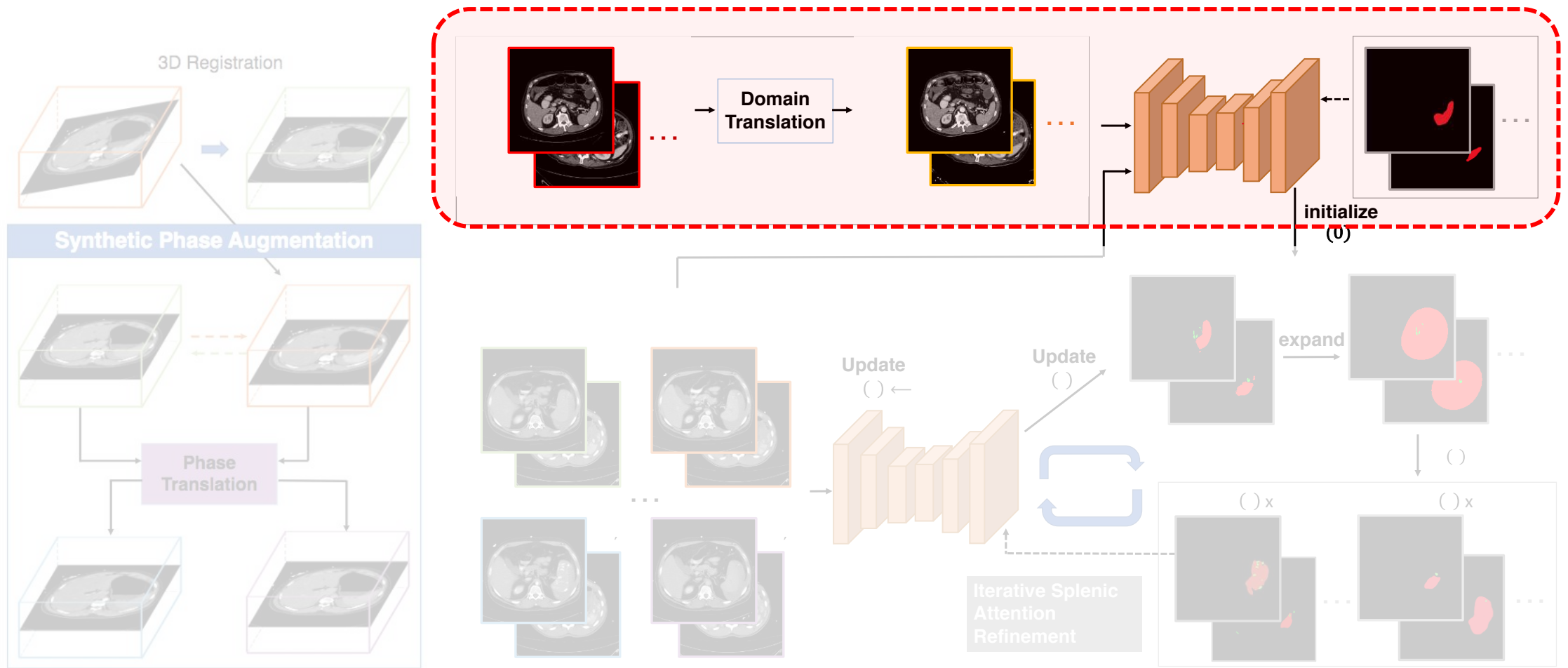
The Proposed Pipeline

- Exploiting spatial priors as external attention



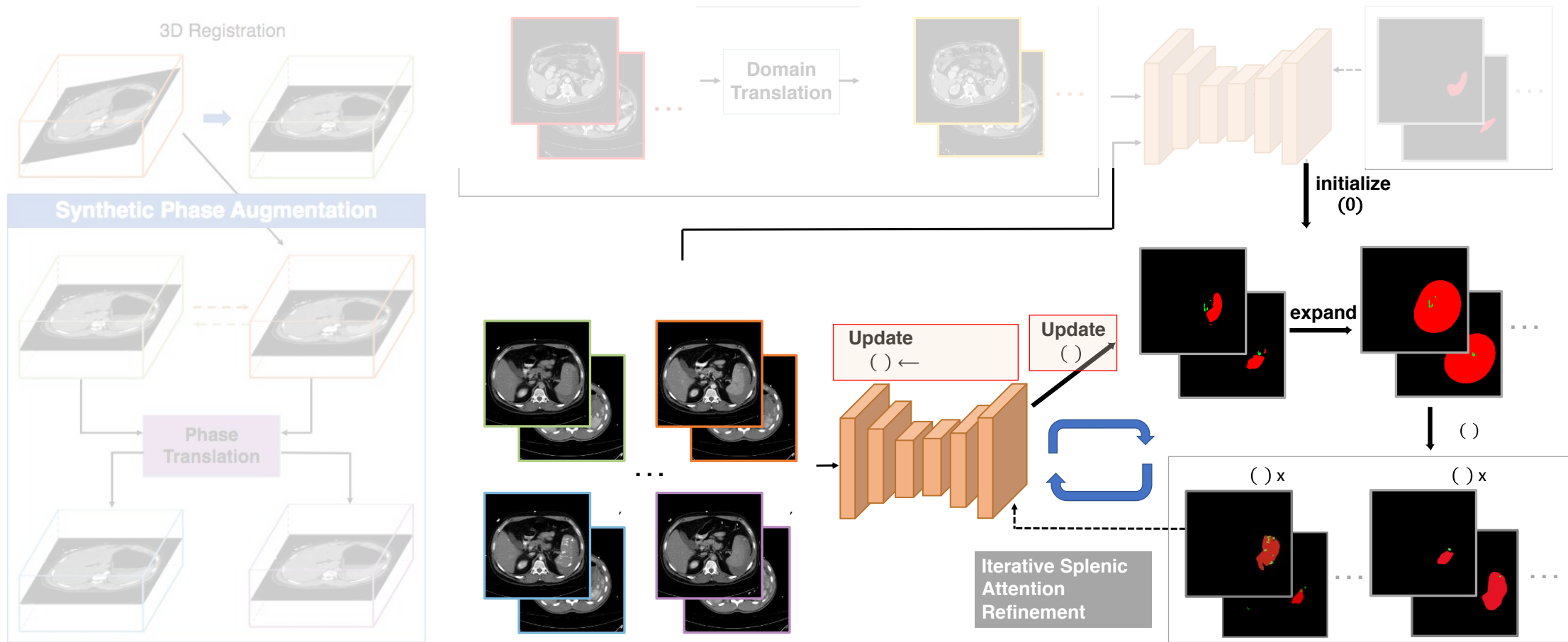
The Proposed Pipeline

- Exploiting spatial priors as external attention



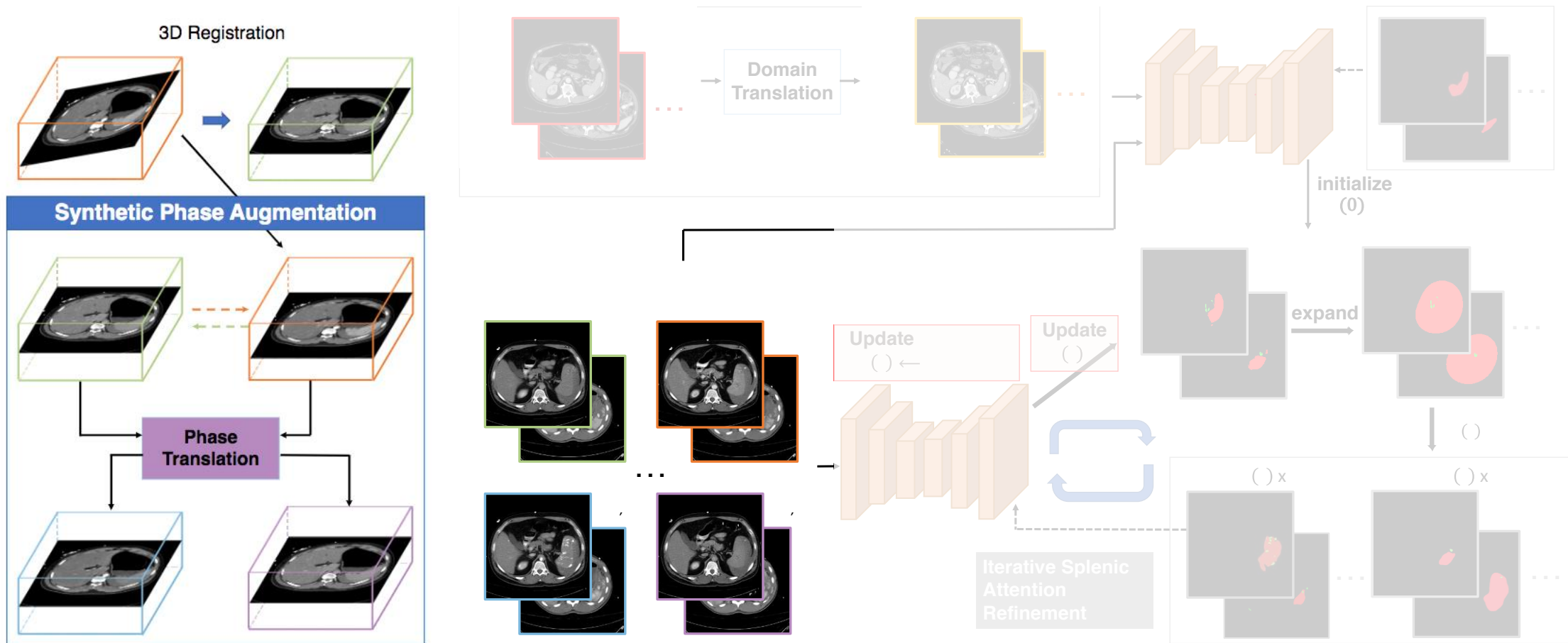
The Proposed Pipeline

- Exploiting spatial priors as external attention



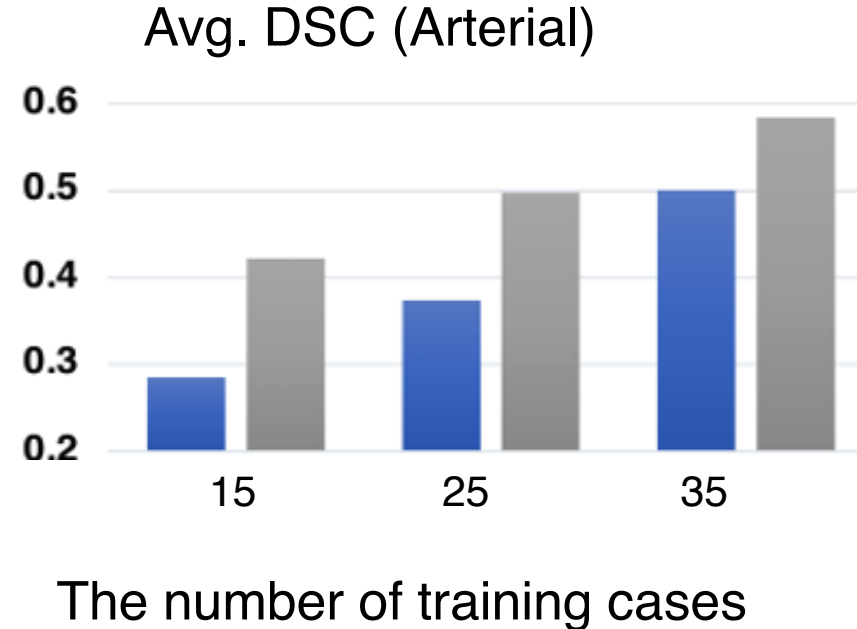
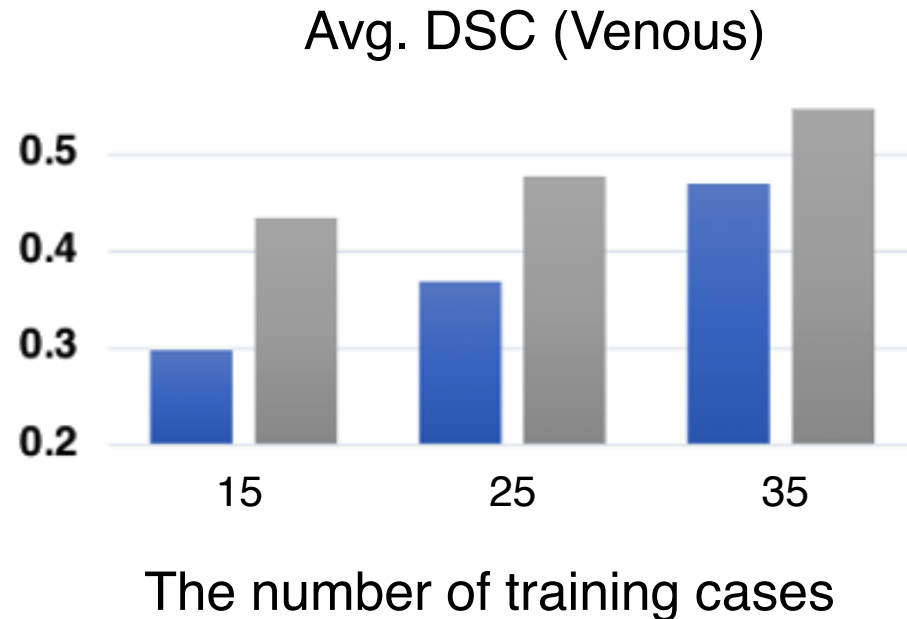
The Proposed Pipeline

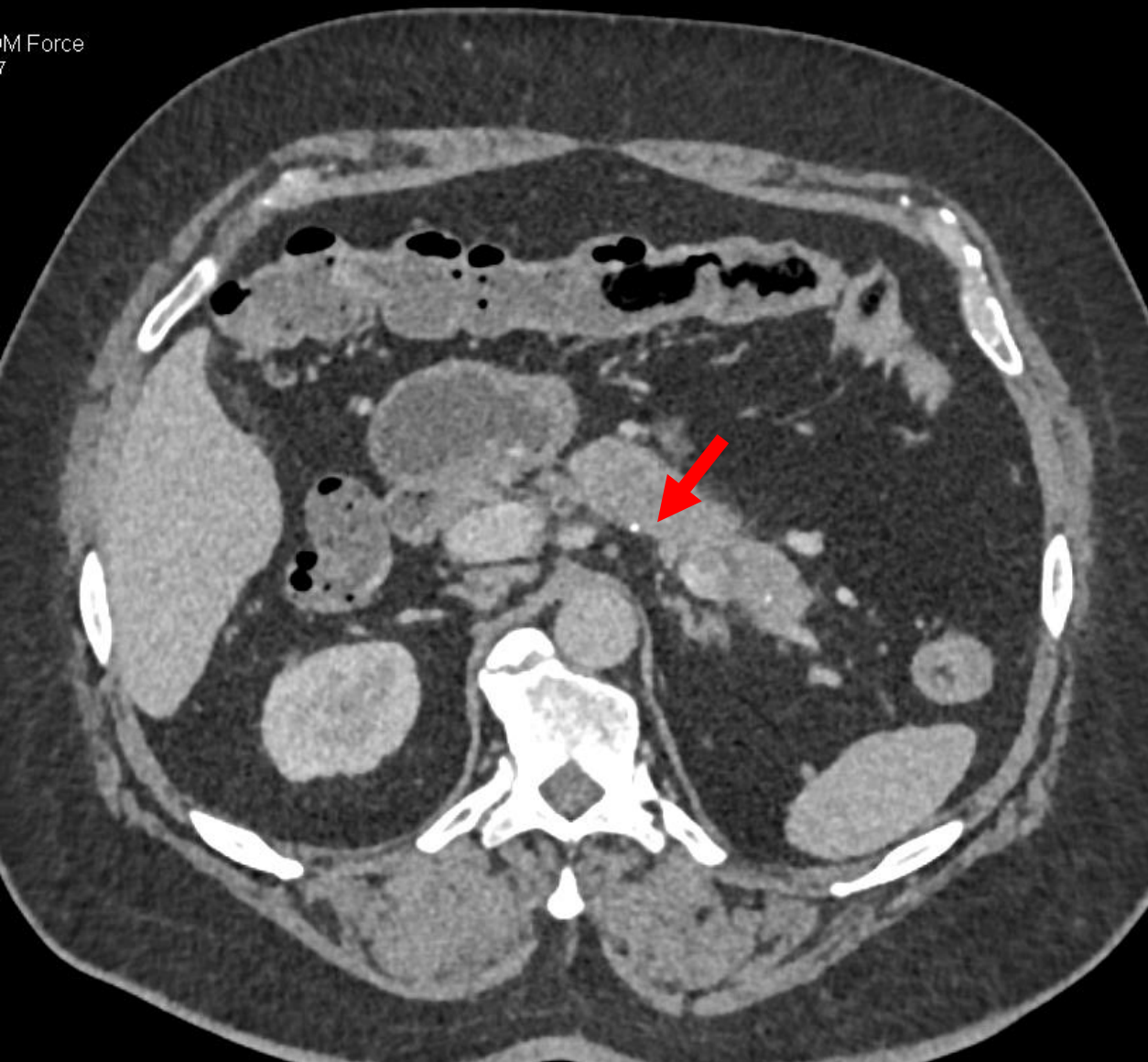
- Exploiting spatial priors as external attention



Experimental Results

- Exploiting spatial priors as external attention
- Results





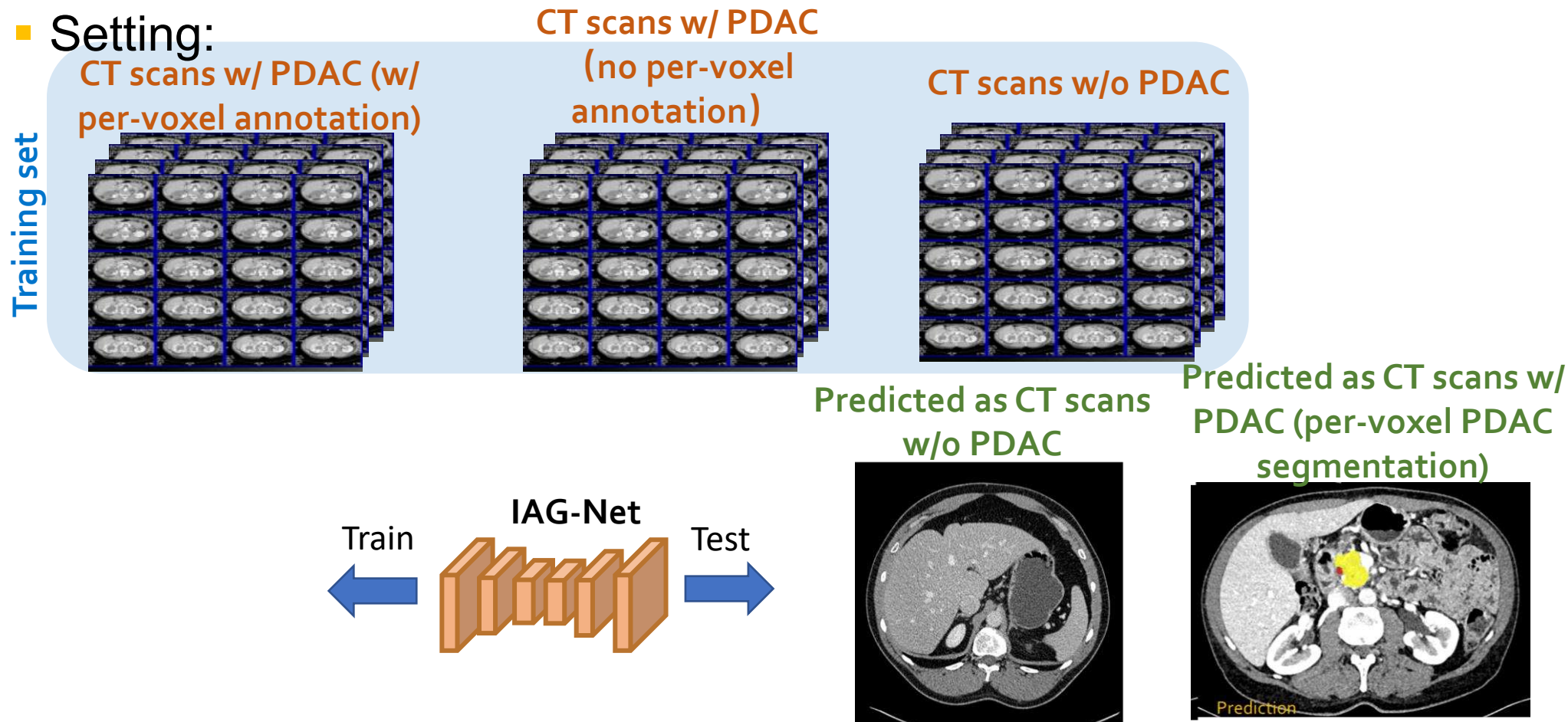
Resectable cancer missed



Unresectable cancer detected later

Pancreatic Ductal Adenocarcinoma Prediction

- Partially supervised attention-guided PDAC prediction
- Setting:



Problems to be Solved

- Normal/abnormal with PDAC classification



Binary classification.

- PDAC segmentation (semi-supervised)

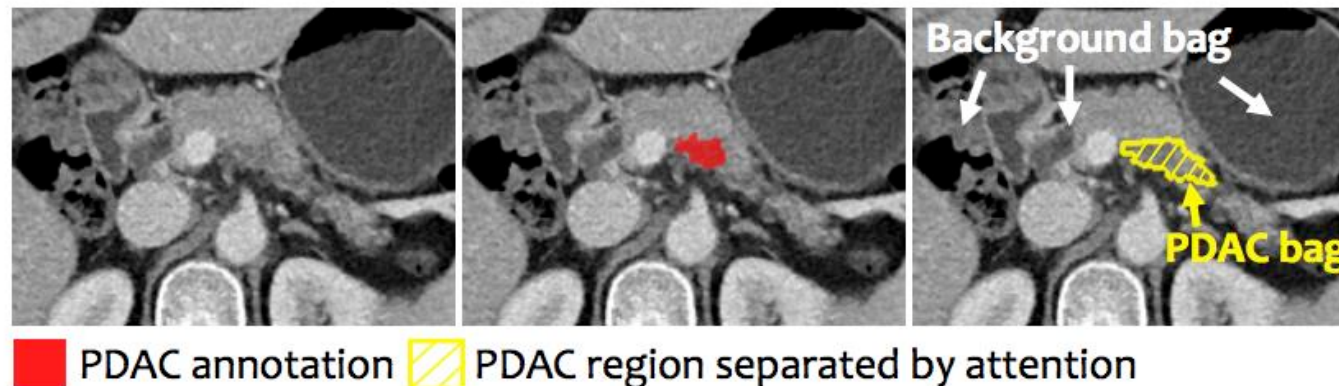


Segmentation.

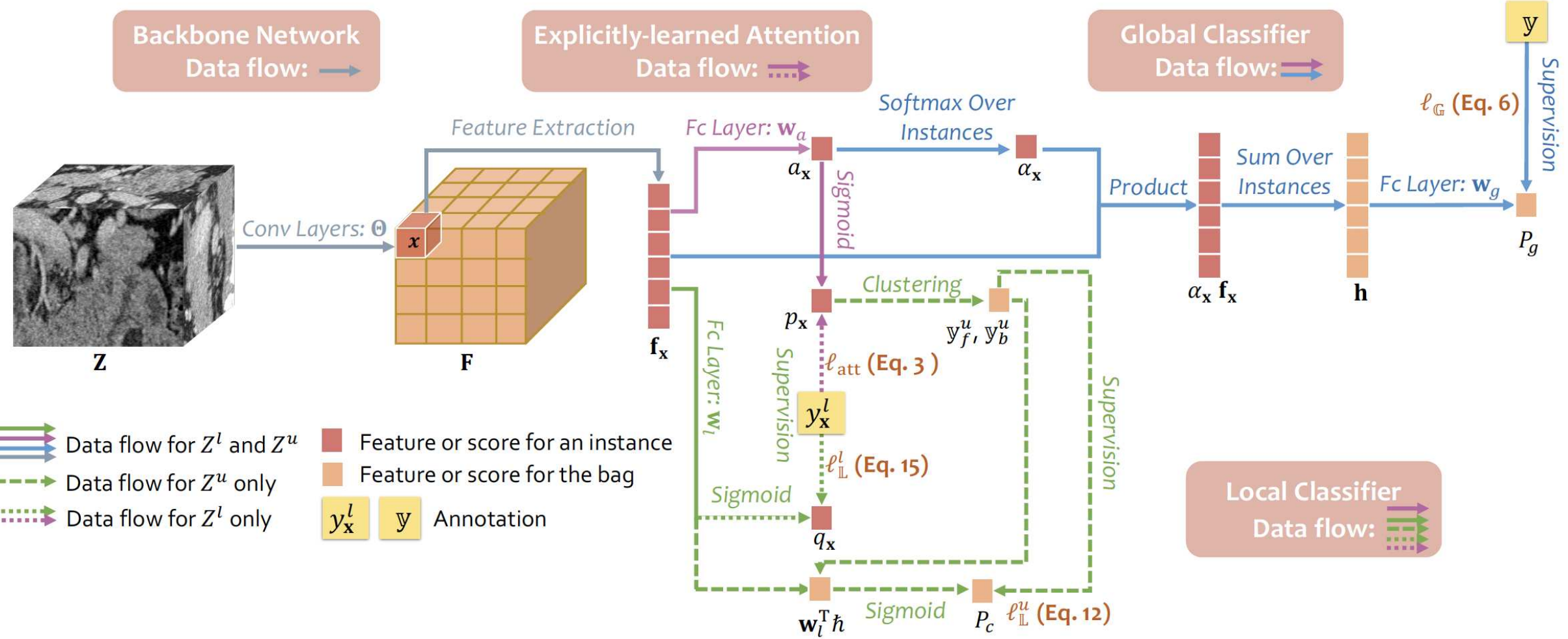


PDAC Classification and Segmentation

- Inductive attention guidance for PDAC prediction
 - For normal/abnormal with PDAC classification, attention -> weight for each instance (voxel) during MIL pooling
 - For semi-supervised PDAC segmentation, attention guidance provides **bag-level pseudo labels** to training data w/o per-voxel PDAC annotation

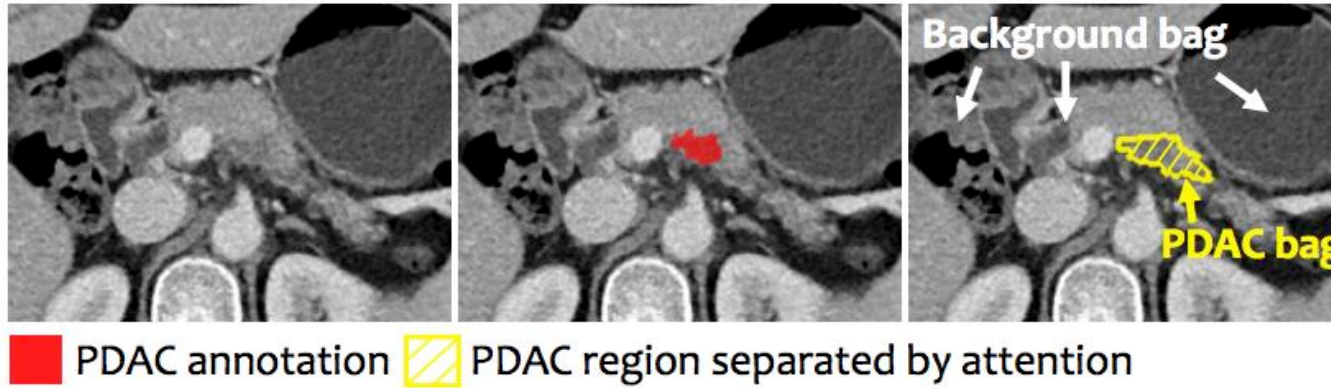


The Proposed Pipeline



Bag-level Pseudo Labels

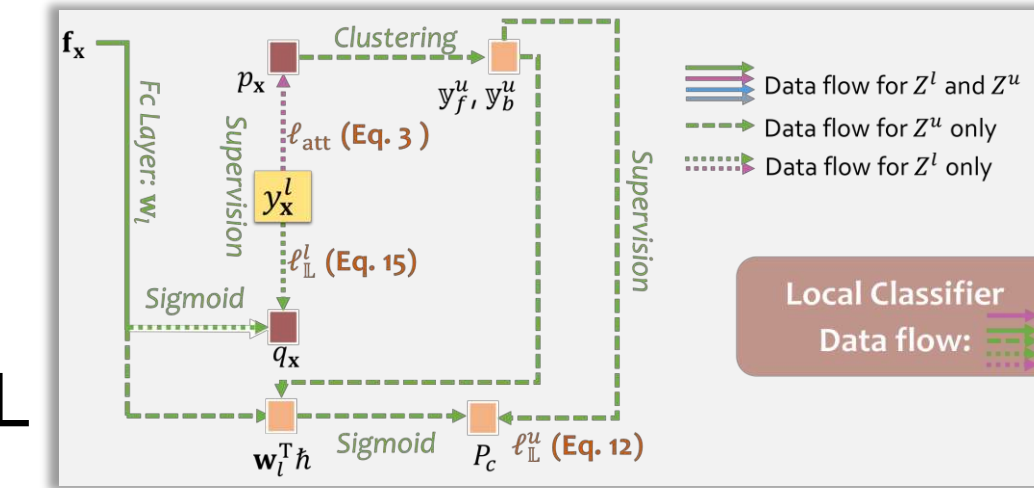
- Learn local instance-level classifier by MIL



Obtain bag-level representation $\mathbf{h}(\mathbf{Z}_b^u)$ and $\mathbf{h}(\mathbf{Z}_f^u)$ by **average pooling**.

Probability that a bag is a PDAC region is obtained through sigmoid operation.

$$\mathbf{w}_l^\top \mathbf{h}(\mathbf{Z}_c^u; \Theta, \mathbf{w}_a) = \frac{1}{|\mathcal{X}_c|} \sum_{\mathbf{x} \in \mathcal{X}_c} \mathbf{w}_l^\top \mathbf{f}_{\mathbf{x}}(\mathbf{Z}^u; \Theta, \mathbf{w}_a)$$



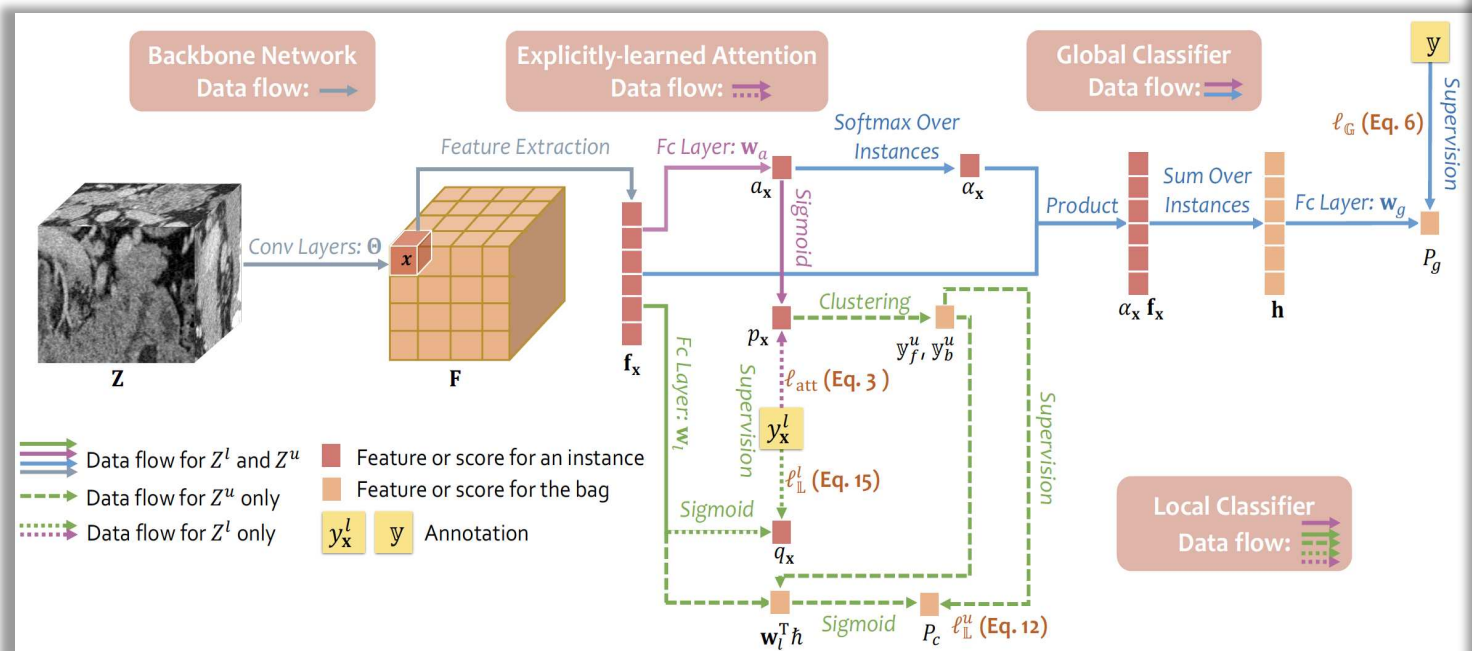
Treat PDAC and background region as small bags:

$$\mathbf{Z}_b^u$$

$$\mathbf{Z}_f^u$$

$$q_{\mathbf{x}}(\mathbf{Z}; \Theta, \mathbf{w}_l) = \frac{1}{1 + \exp(-\mathbf{w}_l^\top \mathbf{f}_{\mathbf{x}}(\mathbf{Z}; \Theta))}$$

Training process of IAG-Net



Input : Training set $\mathcal{D} = \mathcal{D}^l \cup \mathcal{D}^u$, where $\mathcal{D}^l = \{(\mathbf{Z}^l, \mathbf{Y}^l)\}_{l=1}^L$ and $\mathcal{D}^u = \{(\mathbf{Z}^u, \mathbf{y}^u)\}_{u=L+1}^U$; Max number of iterations T ;

Output: Parameters Θ^* , w_a^* , w_l^* and w_g^* ;

```

1  $t \leftarrow 0$ ;
2 Randomly initialize  $\Theta$ ,  $w_a$ ,  $w_l$  and  $w_g$ ;
3 repeat
4    $t \leftarrow t + 1$ ;
5   Randomly select a data sample  $(\mathbf{Z}, \cdot)$  from  $\mathcal{D}$ 
6   if  $(\mathbf{Z}, \cdot) \in \mathcal{D}^l$  then
7     Compute  $\ell_{\text{att}}(\mathbf{Z}^l, \mathbf{Y}^l; \Theta, w_a)$  by Eq. 3 and
8      $\ell_L^l(\mathbf{Z}^l, \mathbf{Y}^l; \Theta, w_l)$  by Eq. 15;
9   else
10    Obtain  $\mathcal{X}_f$  and  $\mathcal{X}_b$  by minimizing Eq. 9
11    Compute  $\ell_L^u(\mathbf{Z}^u; \Theta, w_a, w_l)$  on  $\{\mathcal{X}_f, \mathcal{X}_b\}$  by
12    Eq. 12;
13  end
14  Compute  $\ell_G(\mathbf{Z}, \mathbf{y}; \Theta, w_a, w_g)$  by Eq. 6;
15  Compute  $L_{\text{IAG}}(\mathcal{D}; \Theta, w_a, w_g, w_l)$  by Eq. 19;
16  Update  $\Theta$ ,  $w_a$ ,  $w_l$  and  $w_g$  by Gradient Descent;
17 until  $t = T$ ;
Return:  $(\Theta, w_a, w_l, w_g)^* \leftarrow (\Theta, w_a, w_l, w_g)$ .

```

Experimental Results

Backbone	Method	Mean DSC (Max, Median)	Sensitivity	Specificity	# Parameters
VGG-Net	Attention-based MIL [40]	—	99.00	98.00	14.78M
	FCN-8s [45]	50.02 ± 26.15 (89.75, 56.50)	—	—	134.27M
	Li <i>et al.</i> [18]	41.31 ± 21.41 (82.80, 41.55)	99.00	96.75	14.72M
	DMPCT [19]	49.24 ± 27.04 (90.89, 54.12)	—	—	134.27M
	Collaborative [39]	52.52 ± 19.35 (85.88, 55.37)	98.25	96.75	21.02M
	IAG-Net (Ours)	54.38 ± 18.77 (87.65, 57.00)	99.25	97.50	14.72M
IAG-Net (fully-supervised)		55.45 ± 19.60 (88.36, 58.29)	99.25	97.75	14.72M
U-Net	Attention-based MIL [40]	—	97.00	94.50	30.44M
	U-Net [25]	51.87 ± 25.94 (93.63, 56.52)	—	—	30.43M
	Li <i>et al.</i> [18]	47.91 ± 26.13 (90.84, 51.73)	99.25	93.75	30.43M
	DMPCT [19]	52.35 ± 26.38 (92.23, 56.69)	—	—	30.43M
	Collaborative [39]	55.24 ± 24.96 (93.88, 60.94)	98.75	95.75	36.74M
	IAG-Net (Ours)	60.29 ± 21.60 (94.04 , 64.37)	99.75	96.50	30.43M
IAG-Net (fully-supervised)		60.38 ± 23.83 (93.61, 66.93)	98.25	98.00	30.43M

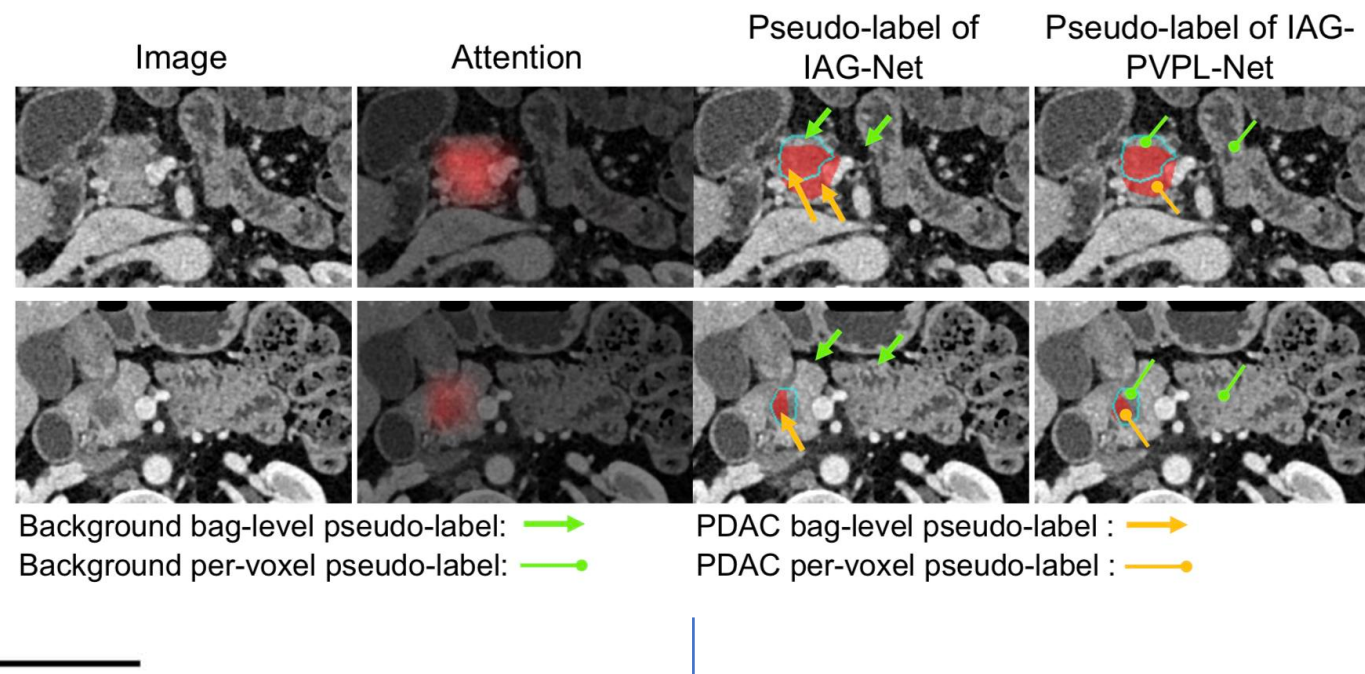
Ablation Study and Discussion

ABALATION ON THE JOINT LEARNING FRAMEWORK.

Global classifier	Local classifier	Mean DSC (Max, Median)	Sens.	Spec.
	✓	51.19 ± 18.49 (86.80, 52.95)	98.00	29.50
✓		6.900 ± 6.100 (47.04, 5.210)	98.00	98.75
✓	✓	54.38 ± 18.77 (87.65, 57.00)	99.25	97.50

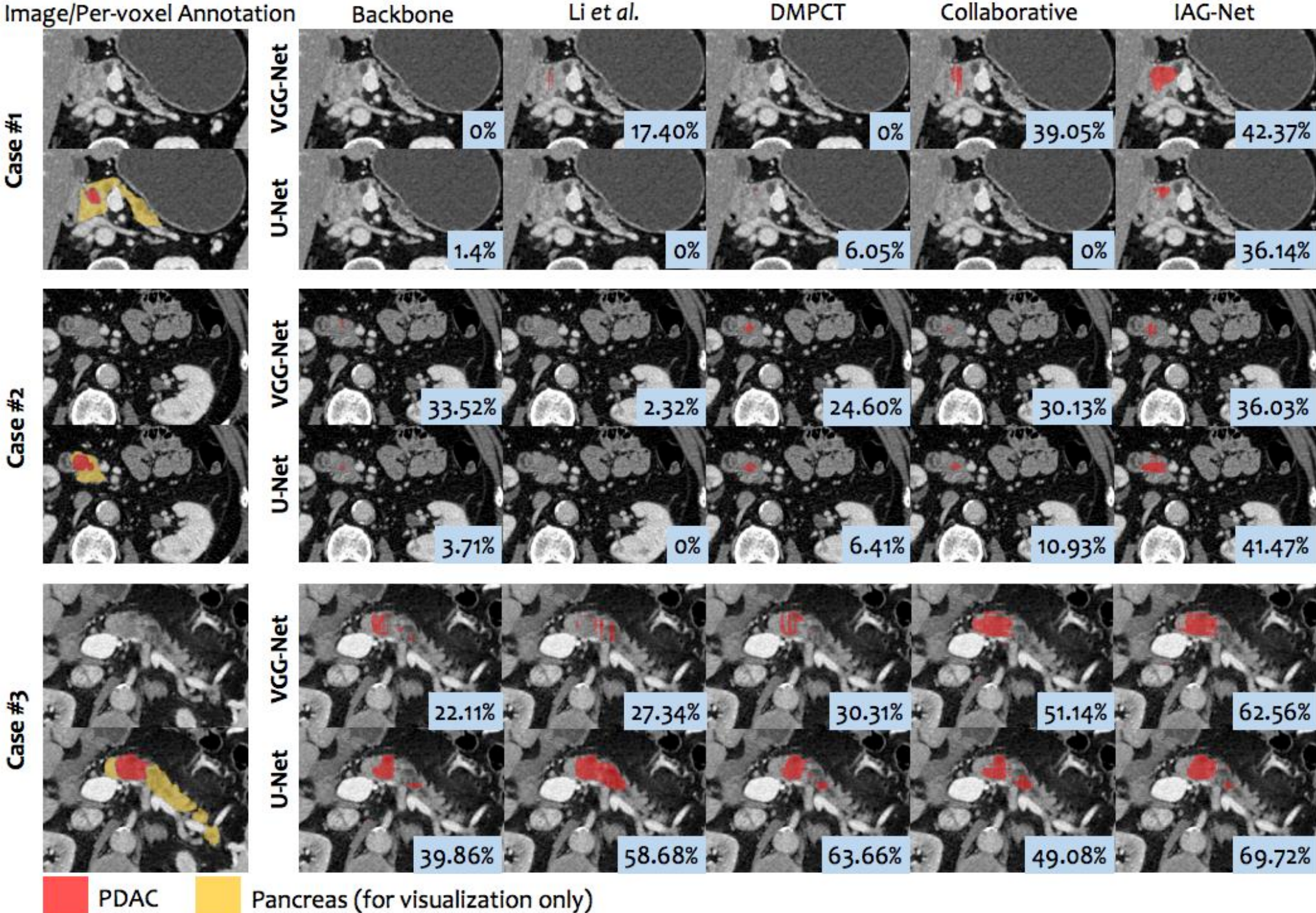
ABALATION STUDY ON THE GLOBAL CLASSIFIER.

MIL method	Mean DSC (Max, Median)	Sens.	Spec.
Max	51.85 ± 20.63 (87.65, 55.21)	98.75	96.50
Average	34.12 ± 19.46 (83.25, 32.91)	86.75	99.75
Attention	54.38 ± 18.77 (87.65, 57.00)	99.25	97.50



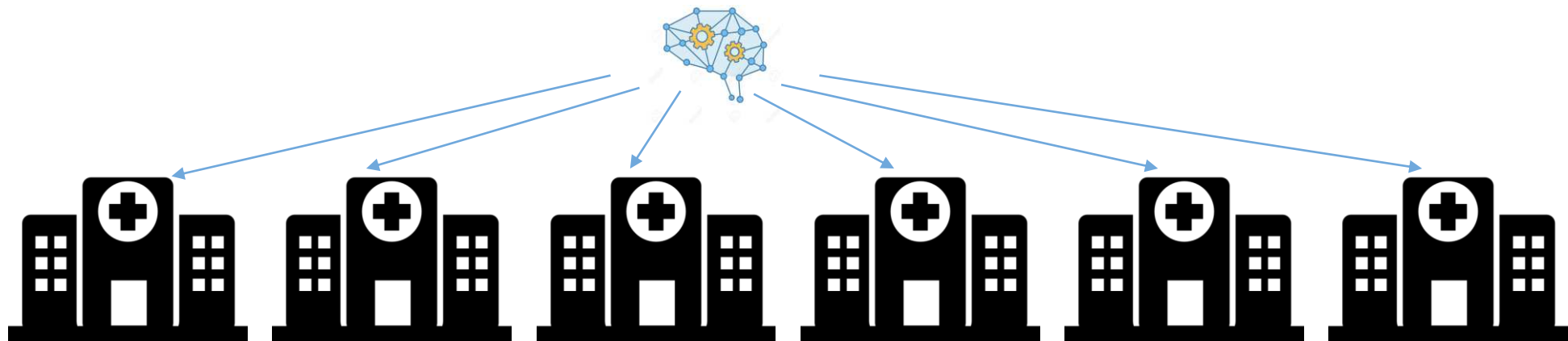
Usually the misclassified instances in a bag are minor, the correctness of the bag-level pseudo-labels can be guaranteed after average pooling.

But the per-voxel pseudo-labels of these instances are treated as noises.



Domain Adaptation on CT Scans

- Generalize the model trained on the internal dataset to external datasets without re-train the model
 - Different scanners / protocols / parameters
 - Different slice thickness & spacing
 - Other dimensions ...
- There is no label available from the external datasets



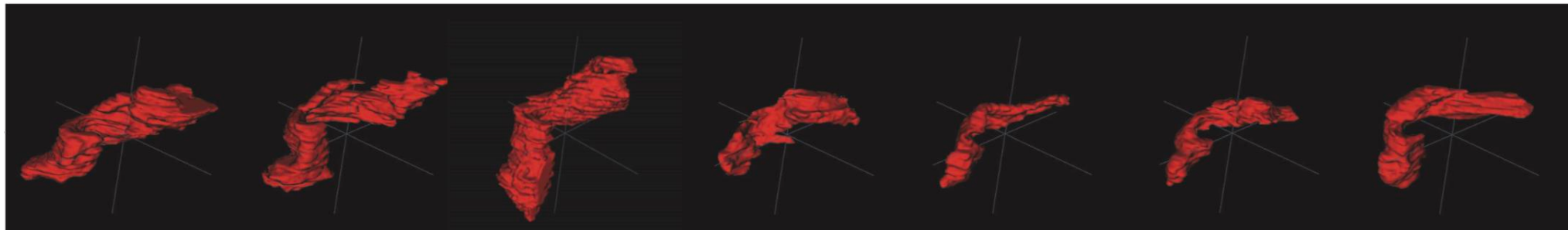
Domain Adaptation on CT Scans

- Data prior:
 - Same organ from different datasets share the same shape distribution
[Unsupervised Domain Adaptation through Shape Modeling for Medical Image Segmentation](#)
 - Multi-organ segmentation: spatial relationship between internal structures are relatively fixed
[Domain Adaptive Relational Reasoning for 3D Multi-Organ Segmentation](#)

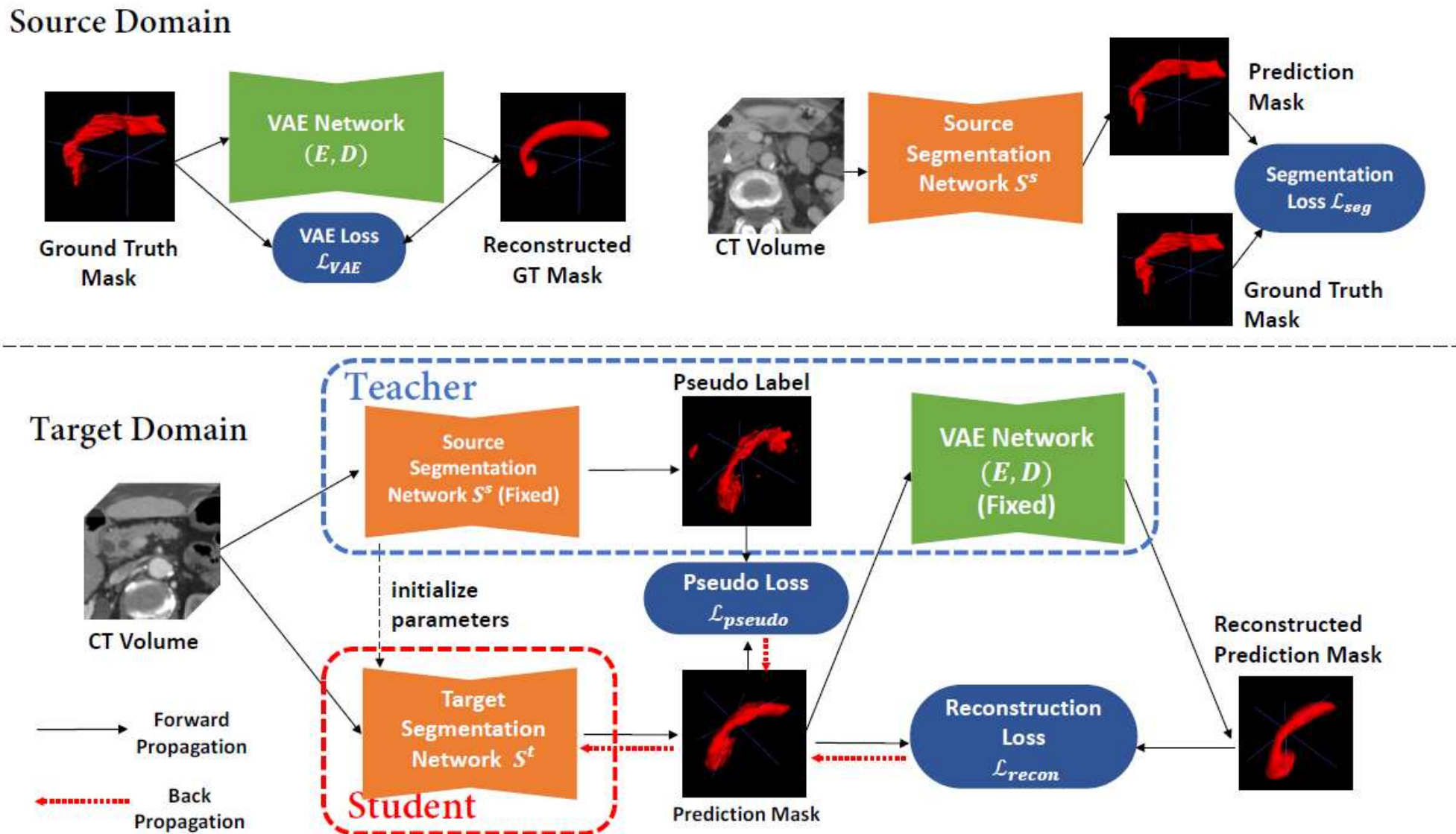
Modeling Shape with Variational Autoencoder

■ Intuition

- Same organ from different datasets shares the same representation of 3D anatomy
- Source domain:
 - use VAE to capture shape statistics. Learn teacher model.
- Domain adaptation:
 - student network is guided by teacher network & VAE reconstruction loss.



Modeling Shape with VAE



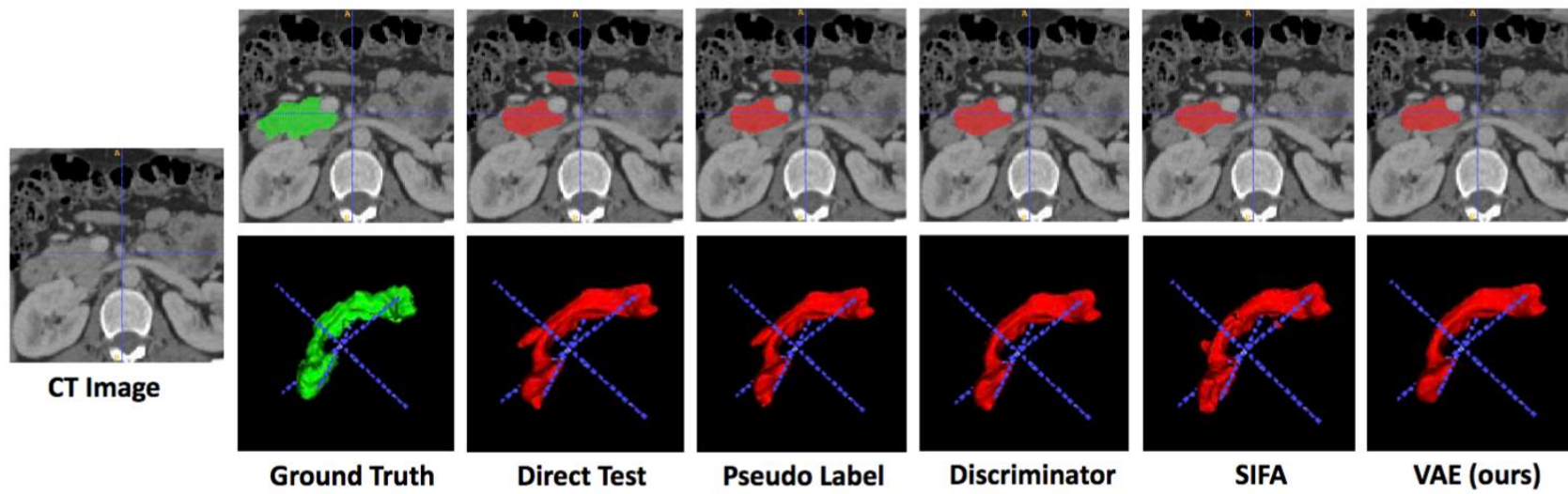
Variational Autoencoder

- Model the shape in VAE
 - Assume normal label y obeys a certain distribution $P(y)$
 - Aim to find an estimation function $Q(z|y)$

$$\log P(y) - \mathcal{KL}[Q(z|y)\|P(z|y)] = \mathbb{E}_{z\sim Q}[\log P(y|z)] - \mathcal{KL}[Q(z|y)\|P(z)]$$

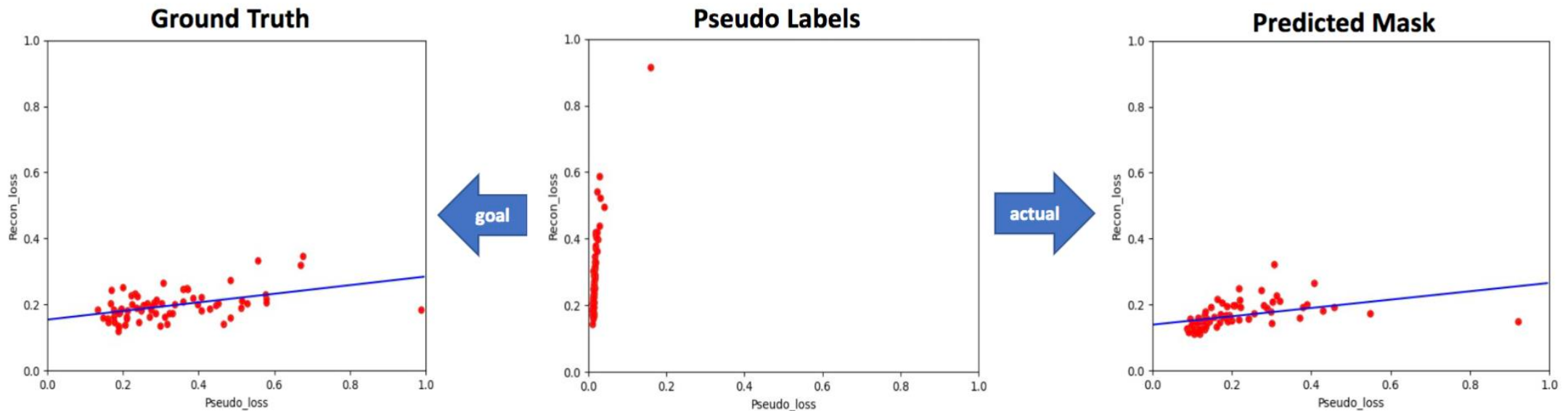
Experiments

Method	MSD		Synapse		In-house IV		In-house Oral	
	Dice	Gap	Dice	Gap	Dice	Gap	Dice	Gap
Direct Test	0.6777	0.1283	0.7452	0.0509	0.7983	0.0657	0.7019	0.1208
Pseudo Label	0.7068	0.0992	0.7769	0.0192	0.8139	0.0501	0.7378	0.0849
Discriminator	0.7176	0.0884	0.7817	0.0144	0.8127	0.0513	0.7296	0.0931
SIFA	0.6605	-	0.7456	-	0.7758	-	0.6910	-
VAE pipeline (ours)	0.7574	0.0486	0.7869	0.0092	0.8264	0.0376	0.7453	0.0774
<i>Upper bound</i>	<i>0.8060</i>	-	<i>0.7961</i>	-	<i>0.8640</i>	-	<i>0.8227</i>	-



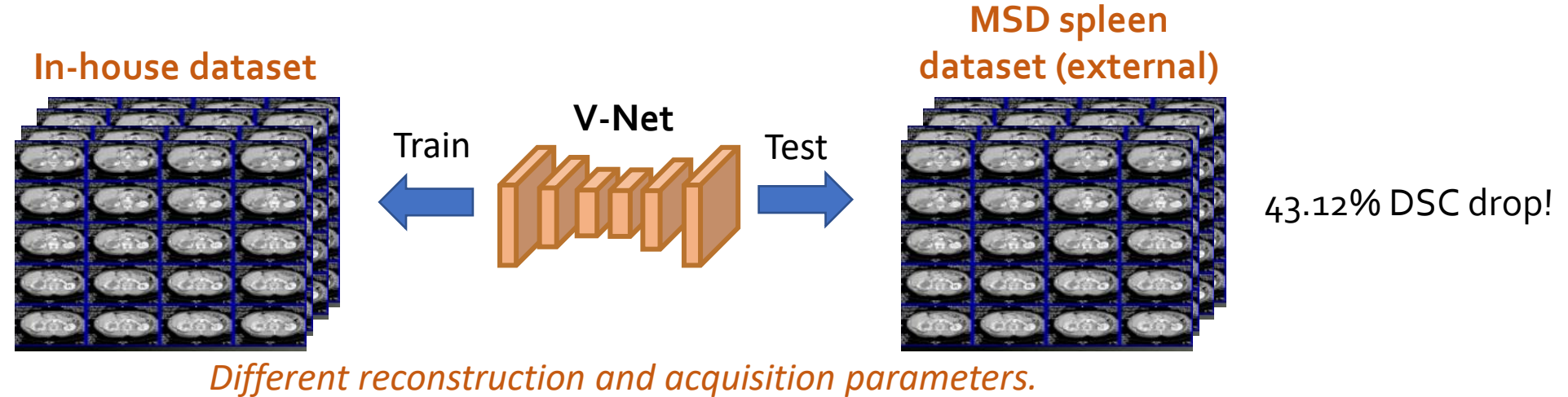
Why it works?

- Validation data from MSD as example.



Domain Adaptation for Multi-organ Segmentation on CT

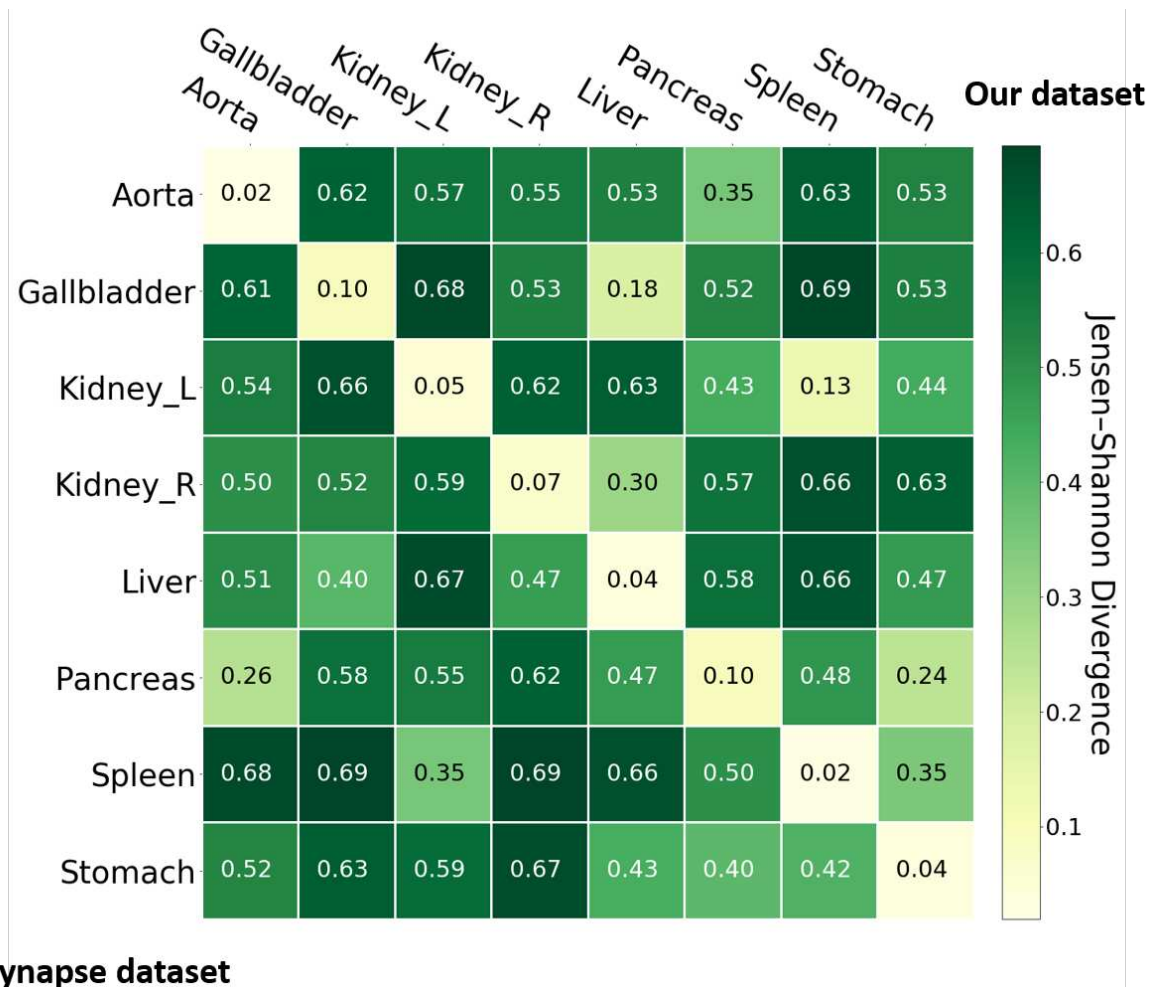
- Performance degradation when transferring domains
 - Due to a high deviation of scanners / protocols / parameters



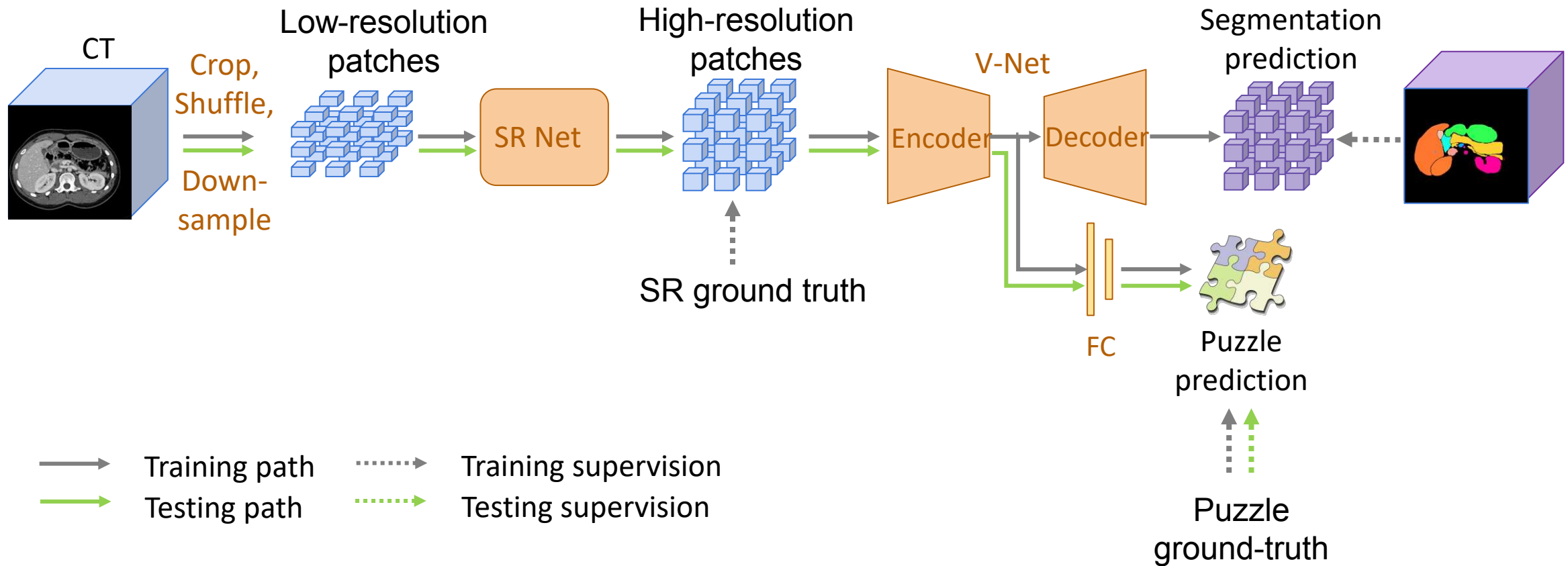
- Large-scale applications: generalization capability to deal with scans acquired with different scanners / protocols as compared to the training data is desirable

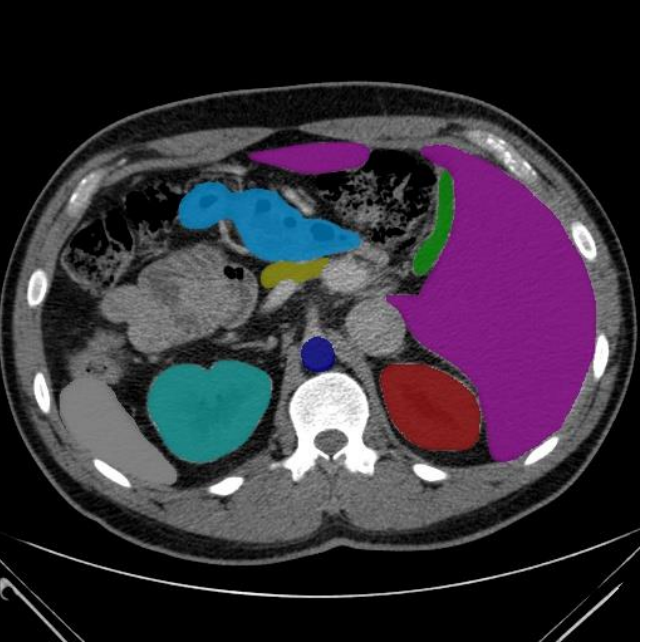
Intuition

- The spatial relationship between internal structures in medical images are relatively fixed.
- JensenShannon divergence matrix of the location probability distribution of the 8 organs between two datasets.
- Co-occurrence of the same organ appearing in the same location is high.

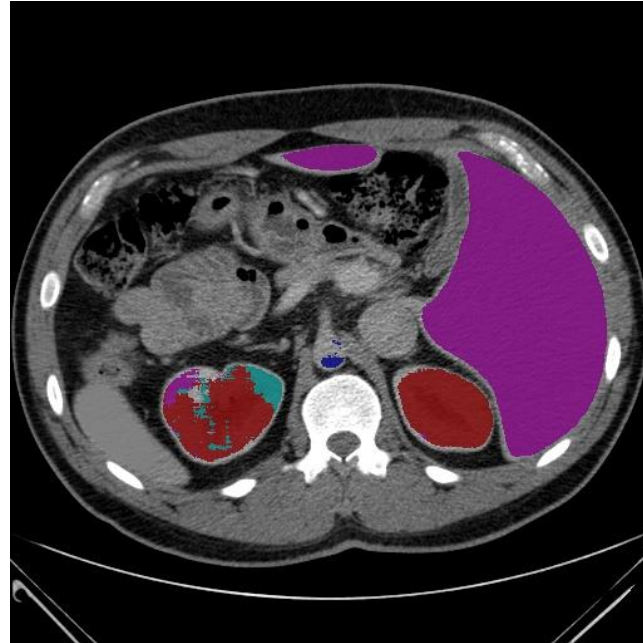


Domain Adaptive Relational Reasoning (DARR) Model Overview

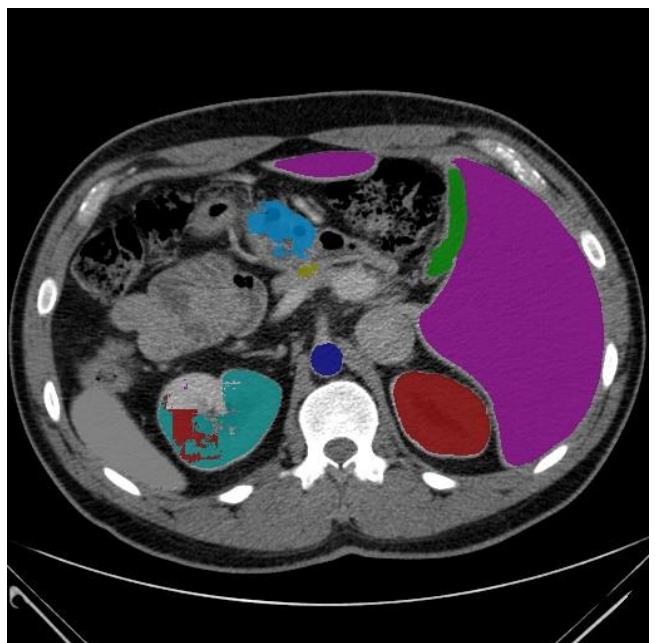




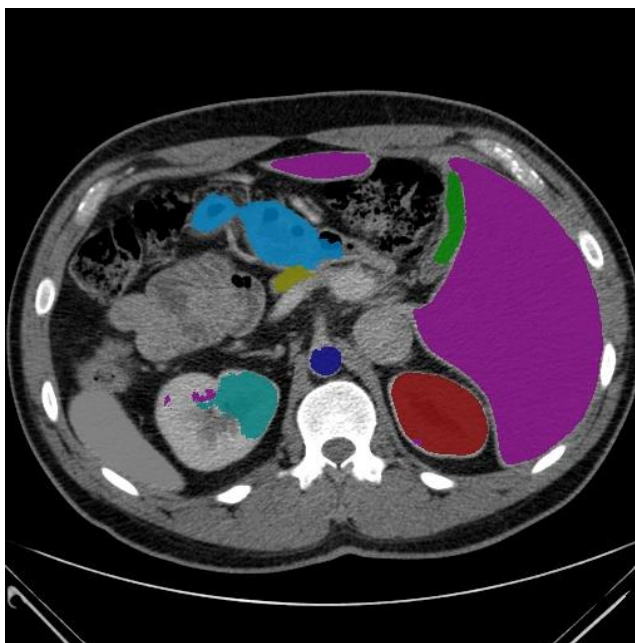
Ground truth



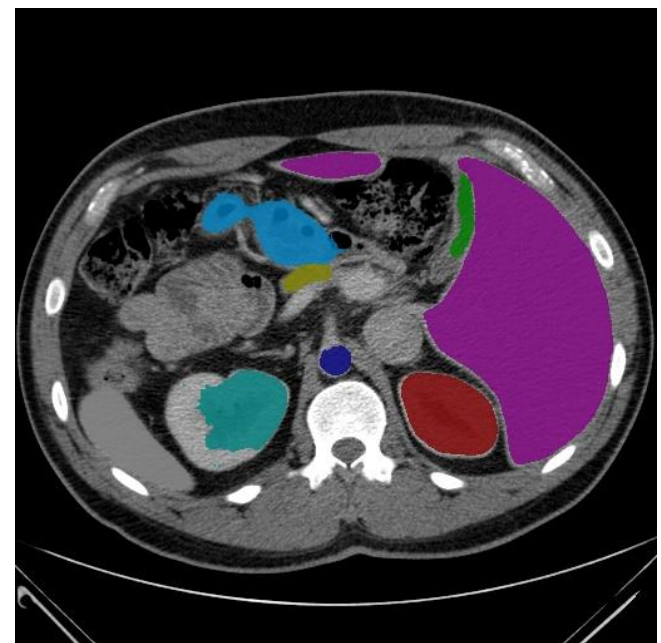
Direct test



VNET-Puzzle



VNET-SR



DARR

Discussions on Super Resolution

- Super-resolution network (SR) boosts the segmentation performance. (52.42% -> 61.27%)
- If the network is not trained with SR, then testing on SR images does not gain improvements
- After trained with SR-Net, a change of up-sampling method does not alter the result too much
- We hypothesize that SR-Net serves as a data augmenter during training

	SR Synapse	Bilinear Synapse	SR FELIX	Bilinear FELIX	Direct on FELIX
Trained with SR	61.27%	60.77%	87.41%	86.52%	84.27%
Trained w/o SR	51.41%	52.42%	-	-	87.85%



JOHNS HOPKINS
UNIVERSITY



Stanford
MEDICINE



UNIVERSITY OF CALIFORNIA
SANTA CRUZ

Thank you!